Modern Journal of Statistics
2(1), 1–31
DOI:https://doi.org/10.64389/mjs.2026.02113
https://sphinxsp.org/journal/index.php/mjs/

Research article

Inference under Hybrid Censoring for the Quadratic Hazard Rate Model: Simulation and Applications to COVID-19 Mortality

Moustafa N. Mousa[1,*], **M. E. Moshref**[2], **N. Youns**[1], **M. M. M. Mansour**[3]

[1] Department of Mathematics, Faculty of Science, Kafrelsheikh University, Kafrelsheikh, 33516, Egypt; mostafa.nabil_a006@sci.kfs.edu.eg; nagwa.elkalakat@sci.kfs.edu.eg

[2] Department of Mathematics, Faculty of Science, Al-Azhar University, Nasr City, 11884, Cairo, Egypt; mmosh399@gmail.com

[3] Department of Basic Science, Faculty of Engineering, The British University in Egypt, El Sherouk City, 11837, Cairo, Egypt; mahmoud.mansour@bue.edu.eg

* **Correspondence:** mostafa.nabil_a006@sci.kfs.edu.eg

ARTICLE INFO

Keywords:
Hybrid Censoring
Quadratic Hazard Rate Model
Maximum Likelihood
Bayesian Estimation
COVID-19

Mathematics Subject Classification:
62F10, 62N01, 62N05

Important Dates:
Received: 14 July 2025
Revised: 27 October 2025
Accepted: 30 October 2025
Online: 5 November 2025

ABSTRACT

This study implements Bayesian along with non-Bayesian approaches to estimate the parameters of the three-parameter quadratic hazard rate distribution using hybrid Type-II censoring. The model expands upon linear hazard rate, exponential, and Rayleigh distributions. In the non-Bayesian framework, point estimates and survival and hazard functions are calculated using maximum likelihood estimation (MLE). Asymptotic confidence intervals are derived, with a focus on the delta method. By applying independent normal and gamma priors, Bayesian inference produces point estimates and credible intervals using different symmetric and asymmetric loss functions. The analytical intractability of posterior distributions makes Markov chain Monte Carlo (MCMC) methods necessary for sampling purposes. The evaluation of point and interval estimates depends on root mean squared error (RMSE) in combination with mean relative absolute bias (MRAB), average confidence interval length (AL), and coverage probability (CP). The performance evaluation through different sample sizes and censoring schemes is conducted by simulation studies, while real-world data from COVID-19 mortality demonstrates the practical implementation of methods. Graphical and numerical analyses confirm the existence and uniqueness of the estimates. Results indicate that Bayesian methods deliver superior accuracy and more robust estimates than their non-Bayesian counterparts for survival analysis purposes in clinical and medical research.

1. Introduction

Clinical and medical research has changed dramatically recently due to the integration of modern scientific advances, computing power, and simulation techniques. Patients have benefited from these advances because they have led to improved disease simulation, improved treatment, and more accurate, effective, and rapid risk assessment. Medical diagnoses, epidemiological research, and healthcare interventions are all constantly being advanced by developments in data science, biostatistics, and computational techniques.

Clinical and medical research often uses data on survival time, that is, time until some event of interest, such as the patient's death. This idea is particularly important in studies where patients are followed for many years to see how long they remain in remission after treatment. For example, diseases like COVID-19 have highlighted the importance of survival analysis, as death rates from the disease vary by age, health, and access to healthcare.

It has been observed that the elderly and people with comorbidities have higher mortality, and thus there is a need to have robust statistical methods to analyze survival patterns and guide healthcare policy development. Readers are encouraged to read the works of Almongy et al. [3], EL-Sagheer et al. [20], Hossam et al. [29], Alghamdi and Abd El-Raouf [2], and Slater et al. [46] for a comprehensive understanding of COVID-19 mortality rates and their analysis.

But ethical issues, time limits, and cost make it often impossible to obtain perfect survival data. Studies may have censored data due to participant withdrawal, shortened follow-up periods, or incomplete knowledge of medical events. To overcome such challenges without reducing the quality of their findings, researchers employ statistical techniques that allow for meaningful deductions from incomplete observations. In survival analysis, censoring methods play a crucial role in the examination of time-to-event data, such as mortality rates, treatment responses, and illness recurrence. These techniques enable researchers to optimize study designs, minimize resource consumption, and derive timely insights without compromising statistical accuracy.

Censoring scheme selection depends on the research objectives alongside study constraints. The conventional Type-I censoring, or time censoring, suspends data collection after a predetermined study duration, while all units not faulty during this time become censored. The specified time limitation for data analysis restricts researchers to studying only data collected before the predefined period, thus potentially leading to biased results.

Additionally, conventional Type-II censoring, or failure censoring, continues the study until a predetermined number of failures is observed, at which point data collection ceases, irrespective of the study's duration. When the study period ends with a limited number of observed events relative to total population units, the obtained data might not accurately represent population statistics. Thus, survival analysis requires different censoring approaches because current methods do not meet the standards of adaptability or efficiency in their analysis.

Research analysts widely utilize the hybrid Type-II censoring scheme (H-T-II CS) as an effective solution to resolve the shortcomings found in these censoring approaches. This scheme optimizes test duration along with data utilization by combining Type-I and Type-II schemes and focuses on the collection of data that corresponds to the maximum time between the occurrence of a predetermined number of failures r, or the specified time τ. In survival studies, this approach enhances parameter estimates. It is frequently used to balance cost, time, and data efficiency in clinical studies, industrial testing, and quality control.

1.1. Model Description and Formulation

Suppose that an experimenter placed a total of n independently and identically distributed (*i.i.d.*) units on a life test simultaneously represented by $y_{i:n}$ for $i = 1, 2, \ldots, n$ and let $y_{i:n}$ represent the i^{th} ordered failure time. But in the context of H-T-II CS, we focus on the dataset corresponding to the maximum time between the occurrence of the r^{th} failure, which is predetermined, or the specified time τ. *i.e.*, the study terminates at max $(y_{r:n}, \tau)$. Hence, the random sample can be drawn from the observations in the following three scenarios:

Case I: $(y_{1:n}, y_{2:n}, y_{3:n}, \ldots, y_{r:n})$ if $\tau < y_{r:n}$.
Case II: $(y_{1:n}, y_{2:n}, y_{3:n}, \ldots, y_{m:n})$ if $\tau \geq y_{r:n}$ and $r \leq m \leq n$.
Case III: $(y_{1:n}, y_{2:n}, y_{3:n}, \ldots, y_{n:n})$ if $\tau \geq y_{n:n}$.

Given these scenarios, if the lifetimes of the observed sample follow a distribution characterized by three parameters (α, β, λ) with probability density function (PDF) $f(y_{i:n}; \alpha, \beta, \lambda)$ and cumulative distribution function (CDF) $F(y_{i:n}; \alpha, \beta, \lambda)$. Therefore, the likelihood function $\mathcal{L} = \mathcal{L}(\alpha, \beta, \lambda \mid \text{data})$ is formulated as:

$$\mathcal{L} = \frac{n!}{(n - r_o)!} \prod_{i=1}^{r_o} f(y_{i:n}; \alpha, \beta, \lambda) \left[1 - F(\tau_o; \alpha, \beta, \lambda)\right]^{n - r_o}, \quad \text{where} \quad \tau_o = \begin{cases} y_{r:n} & \text{if} \quad r_o = r \\ \tau & \text{if} \quad r_o = m \\ y_{n:n} & \text{if} \quad r_o = n \end{cases}. \tag{1.1}$$

Several researchers have contributed to the estimation of unknown parameters under H-T-II CS and a variety of probability distributions. Gupta and Kundu [27] focused on the exponential failure distribution, Childs et al. [14] and Lin et al. [35] focused on the exponential distribution, Kundu [33] focused on Weibull distribution, Banerjee and Kundu [10] focused on the Weibull distribution, Dube et al. [17] focused on the log-normal distribution, Ganguly et al. [24] focused on the two-parameter exponential distribution, Kohansal et al. [31] focused on the weighted exponential distribution, Yadav et al. [49] focused on Marshall-Olkin extended exponential distribution, Liang and Yang [34] focused on exponential distributions, Ateya [7] focused on inverse Weibull distribution, Mansour and Aboshady [37] focused on type -II Gumbel distribution, and Du et al. [16] focused on the power Lindley distribution. There is still a need for more study into new and expanded models, such as the new three-parameter beta distribution proposed by Althubyani et al. [5], the New Power Topp-Leone distribution introduced by Atchadé et al. [6], the Generalized Gudermannian Distribution defined by Rasekhi et al. [43], the extended reduced Kies distribution formulated by Almuqrin et al. [4], and the extended odd Weibull-Lindley distribution by Eissa and Sonar [18] under the H-T-II CS and other censoring schemes, despite these contributions.

Selecting a probability model that accurately reflects the underlying population and captures the characteristics of the observed datasets is crucial before moving forward. This study employs the flexible three-parameter quadratic hazard rate distribution (QHRD), which was first presented by Bain [9]. The QHRD is flexible for modeling lifespan data since it generalizes several well-known distributions. Specifically, it reduces to the linear hazard rate distribution (LHRD) when $\lambda = 0$, simplifies to the exponential distribution (ED) when both $\beta = 0$ and $\lambda = 0$, and becomes the Rayleigh distribution (RD) when $\alpha = 0$ and $\lambda = 0$. It demonstrates an essential benefit because it effectively models different types of hazard function patterns as increasing, decreasing, bathtub-shaped, and inverted bathtub-shaped types. This flexibility makes it applicable to diverse fields, such as figuring out how reliable a product is and testing its life. Elbatal and Butt [21], along with Mustafa [39], Bhatti et al. [12], Merovci and Elbatal [38], Okasha et al. [41], and

Al-Hossain and Dar [1], have conducted studies on the QHRD. However, research into its use under various censoring methods remains limited. This gap is filled by applying QHRD under the H-T-II CS framework. The probability density function (PDF) and the cumulative distribution function (CDF) of a random variable Y following the QHRD are given by:

$$f(y;\alpha,\beta,\lambda) = (\alpha+\beta y+\lambda y^2)e^{-\left(\alpha y+\frac{\beta}{2}y^2+\frac{\lambda}{3}y^3\right)} \quad \text{and} \quad F(y;\alpha,\beta,\lambda) = 1-e^{-\left(\alpha y+\frac{\beta}{2}y^2+\frac{\lambda}{3}y^3\right)}. \tag{1.2}$$

While the survival function (SF) and the hazard function (HF) are given by:

$$S(y;\alpha,\beta,\lambda) = e^{-\left(\alpha y+\frac{\beta}{2}y^2+\frac{\lambda}{3}y^3\right)} \quad \text{and} \quad h(y;\alpha,\beta,\lambda) = \left(\alpha+\beta y+\lambda y^2\right). \tag{1.3}$$

In order to guarantee that $h(y;\alpha,\beta,\lambda) \geq 0$, we restrict the parameter space using $y > 0$, $\alpha \geq 0$, $\lambda \geq 0$, and $\beta \geq -2\sqrt{\alpha\lambda}$. The QHRD has several forms for its SF, HF, CDF, and PDF, as shown in Figure 1.

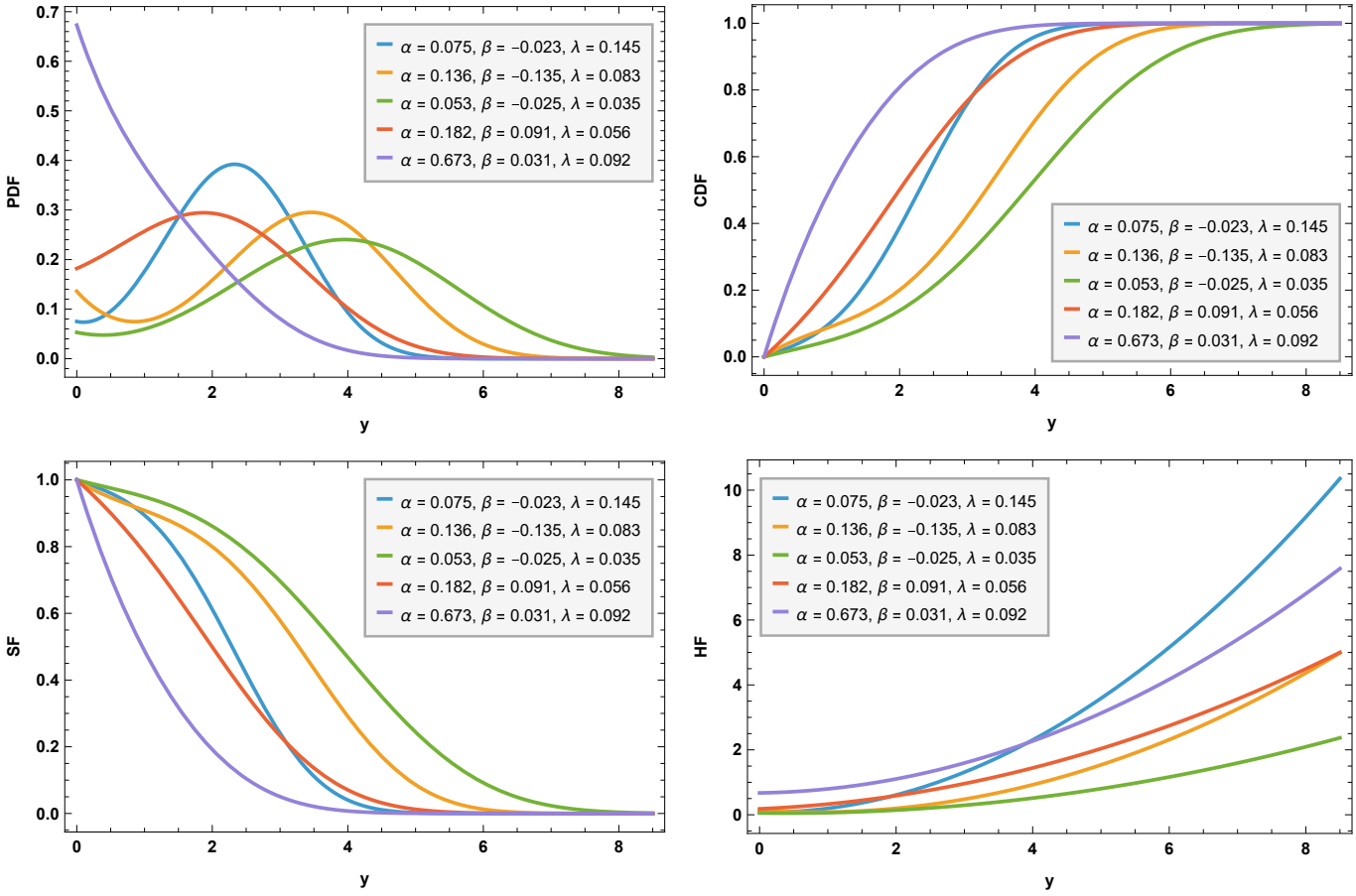

Figure 1. PDF, CDF, SF, and HF of the QHRD.

Our goal is to estimate the parameters of the QHRD under the H-T-II CS. To demonstrate the practical application of our study, we analyze the hazard rate and survival functions using an observed data set that represents the COVID-19 mortality rates. In particular, our research tackles two important questions:

1. What is the probability that a patient with COVID-19 will survive for a given period in the future after diagnosis or hospitalization?

2. If a patient with COVID-19 has survived up to a certain time (e.g., a week after ICU admission), what is the likelihood of deterioration or mortality shortly thereafter?

Answering these questions helps determine the efficacy of the applied treatment program and guide policy decisions for future enhancements. For the estimation of parameters, we employ classical methods, the maximum likelihood (ML), and some Bayesian techniques.

The paper is organized as follows: Section 2 presents the point estimates of the model parameters, along with $S(t)$ and $h(t)$, using the classical (ML) method along with their asymptotic confidence intervals (ACIs). Point and interval estimates through Bayesian approaches with symmetrical and asymmetrical loss functions like the linear exponential, general entropy, and squared error functions appear in Section 3. This section also discusses hyperparameter selection and the application of Markov Chain Monte Carlo (MCMC) techniques. Section 4 conducts a simulation study that evaluates both the accuracy and performance of the obtained estimates. The proposed methods are applied in Section 5 to an actual dataset representing COVID-19 mortality rates to demonstrate their practical utility. Finally, Section 6 summarizes the key findings and their implications.

2. Non-Bayesian Estimation

This section makes use of the ML technique to get the point and the interval estimates of the QHRD parameters (α, β, λ), as well as $S(t)$ and $h(t)$. Interval estimates are obtained from the asymptotic properties of ML. Furthermore, the delta approach is employed for approximating the variances of $S(t)$ and $h(t)$.

2.1. Maximum Likelihood

The ML technique is employed due to its essential properties, such as asymptotic unbiasedness, consistency, efficiency, asymptotic normality, minimum variance, and invariance. According to Eliason [22], Azzalini [8], and Held and Sabanés [28], these characteristics enhance the efficacy of ML as a statistical technique. Consider a H-T-II censored sample $y_{i:n}$ for $i = 1, 2, \ldots, r_o$, with r_o indicating the number of observed units obtained from a lifetime experiment involving n units. These lifetimes follow the QHRD. Thus, the likelihood function $\mathcal{L}$, based on Equations (1.1) and (1.3), is given by:

$$\mathcal{L} = \frac{n!}{(n-r_o)!} \prod_{i=1}^{r_o} \left(\alpha + \beta y_{i:n} + \lambda y_{i:n}^2\right) e^{-\left(\alpha y_{i:n} + \frac{\beta}{2} y_{i:n}^2 + \frac{\lambda}{3} y_{i:n}^3\right)} e^{-(n-r_o)\left(\alpha \tau_o + \frac{\beta}{2}\tau_o^2 + \frac{\lambda}{3}\tau_o^3\right)}. \tag{2.1}$$

The corresponding log-likelihood function is defined as:

$$\ell = \log\left(\frac{n!}{(n-r_o)!}\right) - (n-r_o)\left(\alpha\tau_o + \frac{\beta}{2}\tau_o^2 + \frac{\lambda}{3}\tau_o^3\right) + \sum_{i=1}^{r_o} \log\left(\alpha + \beta y_{i:n} + \lambda y_{i:n}^2\right) - \sum_{i=1}^{r_o}\left(\alpha y_{i:n} + \frac{\beta}{2} y_{i:n}^2 + \frac{\lambda}{3} y_{i:n}^3\right). \tag{2.2}$$

Setting $\frac{\partial \ell}{\partial \alpha}$, $\frac{\partial \ell}{\partial \beta}$, and $\frac{\partial \ell}{\partial \lambda}$ to zero yields the likelihood equation for each parameter. Consequently, the estimation equations for α, β, and λ are given as follows:

$$\frac{\partial \ell}{\partial \alpha} = -(n-r_o)\,\tau_o + \sum_{i=1}^{r_o} \frac{1}{\left(\alpha + \beta y_{i:n} + \lambda y_{i:n}^2\right)} - \sum_{i=1}^{r_o} y_{i:n} = 0, \tag{2.3}$$

$$\frac{\partial \ell}{\partial \beta} = -(n-r_o)\frac{\tau_o^2}{2} + \sum_{i=1}^{r_o}\frac{y_{i:n}}{\left(\alpha+\beta y_{i:n}+\lambda y_{i:n}^2\right)} - \frac{1}{2}\sum_{i=1}^{r_o} y_{i:n}^2 = 0, \tag{2.4}$$

and

$$\frac{\partial \ell}{\partial \lambda} = -(n-r_o)\frac{\tau_o^3}{3} + \sum_{i=1}^{r_o}\frac{y_{i:n}^2}{\left(\alpha+\beta y_{i:n}+\lambda y_{i:n}^2\right)} - \frac{1}{3}\sum_{i=1}^{r_o} y_{i:n}^3 = 0. \tag{2.5}$$

Equations (2.3), (2.4), and (2.5) present a non-linear system, which makes it extremely difficult to derive exact analytical solutions for the variables (α,β,λ). Using the Newton-Raphson algorithm described by EL-Sagheer et al. [19], we solve the non-linear equations numerically to obtain the MLEs represented by $(\hat{\alpha}_{ML},\hat{\beta}_{ML},\hat{\lambda}_{ML}) = \left(\hat{\alpha},\hat{\beta},\hat{\lambda}\right)$. The second partial derivatives mentioned in subsection 2.2 help establish the accuracy of maxima calculations and verify that solutions meet required criteria for distributions with multiple parameters. Mathematica, Maple, and R represent software options that substitute for the use of Newton-Raphson methods in solution approximation. The MLEs of $S(t)$ and $h(t)$ are given by replacing (α,β,λ) by $\left(\hat{\alpha},\hat{\beta},\hat{\lambda}\right)$, utilizing the invariance property in the following manner:

$$\hat{S}(t) = e^{-\left(\hat{\alpha}t+\frac{\hat{\beta}}{2}t^2+\frac{\hat{\lambda}}{3}t^3\right)} \quad \text{and} \quad \hat{h}(t) = \left(\hat{\alpha}+\hat{\beta}t+\hat{\lambda}t^2\right).$$

2.2. *Asymptotic Confidence Intervals*

The asymptotic confidence intervals (ACIs) for the estimators are derived under the assumption of asymptotic normality using the Fisher Information Matrix (FIM), which quantifies the information that the observed data provide about the parameters. The FIM must be inverted to obtain the asymptotic variances and covariances for these parameter MLEs.

$$\mathcal{I}_{ij}(\Theta) = E\left[-\frac{\partial^2 \ell(\Theta)}{\partial\theta_i\partial\theta_j}\right],$$

where $i,j = 1,2,3$ and $\Theta = (\theta_1,\theta_2,\theta_3) = (\alpha,\beta,\lambda)$. The derivation of exact analytical solutions is challenging for these expectations. Therefore, to construct the ACIs for the parameters, we use the observed FIM given by

$$\hat{\mathcal{I}}_{ij}(\Theta) = \left[-\frac{\partial^2 \ell(\Theta)}{\partial\theta_i\partial\theta_j}\right]_{\Theta=\hat{\Theta}}.$$

Consequently, the inverse of the observed FIM for MLEs is expressed as:

$$\hat{\mathcal{F}}\left(\hat{\Theta}\right) = \hat{\mathcal{I}}^{-1}\left(\hat{\alpha},\hat{\beta},\hat{\lambda}\right) = \begin{pmatrix} -\frac{\partial^2\ell}{\partial\alpha^2} & -\frac{\partial^2\ell}{\partial\alpha\partial\beta} & -\frac{\partial^2\ell}{\partial\alpha\partial\lambda} \\ -\frac{\partial^2\ell}{\partial\beta\partial\alpha} & -\frac{\partial^2\ell}{\partial\beta^2} & -\frac{\partial^2\ell}{\partial\beta\partial\lambda} \\ -\frac{\partial^2\ell}{\partial\lambda\partial\alpha} & -\frac{\partial^2\ell}{\partial\lambda\partial\beta} & -\frac{\partial^2\ell}{\partial\lambda^2} \end{pmatrix}^{-1}_{(\alpha,\beta,\lambda)=\left(\hat{\alpha},\hat{\beta},\hat{\lambda}\right)} = \begin{pmatrix} \hat{\sigma}^2_{\hat{\alpha}} & \hat{\sigma}_{\hat{\alpha}\hat{\beta}} & \hat{\sigma}_{\hat{\alpha}\hat{\lambda}} \\ \hat{\sigma}_{\hat{\alpha}\hat{\beta}} & \hat{\sigma}^2_{\hat{\beta}} & \hat{\sigma}_{\hat{\beta}\hat{\lambda}} \\ \hat{\sigma}_{\hat{\alpha}\hat{\lambda}} & \hat{\sigma}_{\hat{\beta}\hat{\lambda}} & \hat{\sigma}^2_{\hat{\lambda}} \end{pmatrix},$$

where

$$\frac{\partial^2\ell}{\partial\hat{\alpha}^2} = -\sum_{i=1}^{r_o}\frac{1}{\left(\hat{\alpha}+\hat{\beta}y_{i:n}+\hat{\lambda}y_{i:n}^2\right)^2}, \quad \frac{\partial^2\ell}{\partial\hat{\alpha}\partial\hat{\beta}} = -\sum_{i=1}^{r_o}\frac{y_{i:n}}{\left(\hat{\alpha}+\hat{\beta}y_{i:n}+\hat{\lambda}y_{i:n}^2\right)^2}, \quad \frac{\partial^2\ell}{\partial\hat{\beta}\partial\hat{\lambda}} = -\sum_{i=1}^{r_o}\frac{y_{i:n}^3}{\left(\hat{\alpha}+\hat{\beta}y_{i:n}+\hat{\lambda}y_{i:n}^2\right)^2},$$

$$\frac{\partial^2 \ell}{\partial \hat{\lambda}^2} = -\sum_{i=1}^{r_o} \frac{y_{i:n}^4}{\left(\hat{\alpha} + \hat{\beta} y_{i:n} + \hat{\lambda} y_{i:n}^2\right)^2}, \quad \text{and} \quad \frac{\partial^2 \ell}{\partial \hat{\alpha} \partial \hat{\lambda}} = \frac{\partial^2 \ell}{\partial \hat{\beta}^2} = -\sum_{i=1}^{r_o} \frac{y_{i:n}^2}{\left(\hat{\alpha} + \hat{\beta} y_{i:n} + \hat{\lambda} y_{i:n}^2\right)^2}.$$

Under the regular assumptions, it is established that the estimates $\left(\hat{\alpha}, \hat{\beta}, \hat{\lambda}\right)$ follow an approximately normal distribution with means (α, β, λ) and a covariance matrix given by $\hat{\mathcal{F}}\left(\hat{\Theta}\right)$. As a result, the $100(1-\gamma)\%$ two-sided ACIs for the MLEs are computed as follows:

$$\left(\hat{\theta}_{i_L}, \hat{\theta}_{i_U}\right) = \left(\hat{\theta}_i - z_{\frac{\gamma}{2}} \hat{\sigma}_{\hat{\theta}_i}, \hat{\theta}_i + z_{\frac{\gamma}{2}} \hat{\sigma}_{\hat{\theta}_i}\right), \text{ for } i = 1, 2, 3.$$

where $\hat{\theta}_{i_L}$ and $\hat{\theta}_{i_U}$ represent the lower and upper confidence limits, respectively. The term $\hat{\sigma}^2_{\hat{\theta}_i}$ denotes the asymptotic variance of $\hat{\theta}_i$, which is derived from $\hat{\mathcal{F}}\left(\hat{\Theta}\right)$, and the percentile of the standard normal distribution is $z_{\frac{\gamma}{2}}$ based on $\frac{\gamma}{2}$ right-tail probability.

In order to get the ACIs for $S(t)$ and $h(t)$, it is essential to determine their variances. The delta approach is employed to estimate the variances of $\hat{S}(t)$ and $\hat{h}(t)$. Greene [26] defined the delta approach as a standard methodology to calculate ACIs for functions of MLEs. This approach approximates the variances of $\hat{S}(t)$ and $\hat{h}(t)$ employing the following relation:

$$\hat{\sigma}^2_{\hat{S}(t)} = \left[\nabla \hat{S}(t)\right]^T \left[\hat{\mathcal{F}}\right] \left[\nabla \hat{S}(t)\right] \quad \text{and} \quad \hat{\sigma}^2_{\hat{h}(t)} = \left[\nabla \hat{h}(t)\right]^T \left[\hat{\mathcal{F}}\right] \left[\nabla \hat{h}(t)\right],$$

where

$$\nabla \hat{S}(t) = \left(\frac{\partial \hat{S}(t)}{\partial \hat{\alpha}}, \frac{\partial \hat{S}(t)}{\partial \hat{\beta}}, \frac{\partial \hat{S}(t)}{\partial \hat{\lambda}}\right) \quad \text{and} \quad \nabla \hat{h}(t) = \left(\frac{\partial \hat{h}(t)}{\partial \hat{\alpha}}, \frac{\partial \hat{h}(t)}{\partial \hat{\beta}}, \frac{\partial \hat{h}(t)}{\partial \hat{\lambda}}\right).$$

Subsequently, the $100(1-\gamma)\%$ two-sided ACIs for $S(t)$ and $h(t)$ can be computed using:

$$\left(\hat{S}(t)_L, \hat{S}(t)_U\right) = \left(\hat{S}(t) - z_{\frac{\gamma}{2}} \hat{\sigma}_{\hat{S}(t)}, \hat{S}(t) + z_{\frac{\gamma}{2}} \hat{\sigma}_{\hat{S}(t)}\right) \quad \text{and} \quad \left(\hat{h}(t)_L, \hat{h}(t)_U\right) = \left(\hat{h}(t) - z_{\frac{\gamma}{2}} \hat{\sigma}_{\hat{h}(t)}, \hat{h}(t) + z_{\frac{\gamma}{2}} \hat{\sigma}_{\hat{h}(t)}\right).$$

3. Bayesian Estimation

Bayesian methodology regards parameters as random variables. A joint prior distribution is constructed to represent prior knowledge before the observation of failure data exists. The approach benefits situations with scarce data because it enables researchers to include their existing knowledge about the topic. To obtain the Bayesian estimators (BEs) for α, β, and λ, as well as $S(t)$ and $h(t)$, assume independent prior distributions for the parameters. Specifically, α and λ follow informative gamma priors, Gamma(μ_i, ν_i), where $\mu_i, \nu_i > 0$ for $i = 1, 3$. Meanwhile, let β be assigned an informative prior Normal(μ_2, ν_2^2) with $\mu_2 \in \mathbb{R}$ and $\nu_2^2 > 0$. This choice allows belief updating with computational feasibility in Bayesian analysis under independence of each parameter. The corresponding probability density functions (PDFs) are given by:

$$\left.\begin{aligned} \pi_1(\alpha) &= \frac{\nu_1^{\mu_1}}{\Gamma(\mu_1)} \alpha^{\mu_1 - 1} e^{-\nu_1 \alpha}, \quad \alpha \geqslant 0, \\ \pi_2(\beta) &= \frac{1}{\sqrt{2\pi\nu_2^2}} e^{-\frac{(\beta-\mu_2)^2}{2\nu_2^2}}, \quad \beta \geqslant -2\sqrt{\alpha\lambda}, \text{ and} \\ \pi_3(\lambda) &= \frac{\nu_3^{\mu_3}}{\Gamma(\mu_3)} \lambda^{\mu_3 - 1} e^{-\nu_3 \lambda}, \quad \lambda \geqslant 0. \end{aligned}\right\} \tag{3.1}$$

Here, $\mu_1, \mu_2, \mu_3, \nu_1, \nu_2^2$, and ν_3 are known as hyperparameters. Consequently, the joint prior distribution of the parameters could possibly be derived using proportionality as follows:

$$\pi(\alpha, \beta, \lambda) \propto \alpha^{\mu_1 - 1} \lambda^{\mu_3 - 1} e^{-\left[\nu_1 \alpha + \frac{(\beta-\mu_2)^2}{2\nu_2^2} + \nu_3 \lambda\right]}, \tag{3.2}$$

where $\mu_1, \mu_3, \nu_1, \nu_3 > 0, \mu_2 \in \mathbb{R}$, and $\nu_2^2 > 0$. The joint posterior distribution of α, β, and λ under $\mathcal{L}$ is derived by combining Equations (2.1) and (3.2) with each other in the following manner:

$$\pi^*(\alpha,\beta,\lambda \mid data) = \mathcal{A}^{-1}\mathcal{L}(\alpha,\beta,\lambda \mid data)\ \pi(\alpha,\beta,\lambda), \tag{3.3}$$

where

$$\mathcal{A} = \int_0^\infty \int_0^\infty \int_{-2\sqrt{\alpha\lambda}}^\infty \mathcal{L}(\alpha,\beta,\lambda \mid \text{data})\ \pi(\alpha,\beta,\lambda)\ d\beta d\alpha d\lambda.$$

Based on Equations (3.2) and (3.3), $\pi^*(\alpha,\beta,\lambda \mid data)$ could possibly be derived using proportionality as follows:

$$\pi^*(\alpha,\beta,\lambda \mid data) \propto \alpha^{\mu_1-1}\lambda^{\mu_3-1}e^{-\left[\nu_1\alpha+\frac{(\beta-\mu_2)^2}{2\nu_2^2}+\nu_3\lambda\right]} \times \prod_{i=1}^{r_o}\left(\alpha+\beta y_{i:n}+\lambda y_{i:n}^2\right)e^{-\left(\alpha y_{i:n}+\frac{\beta}{2}y_{i:n}^2+\frac{\lambda}{3}y_{i:n}^3\right)}$$
$$\times e^{-(n-r_o)\left(\alpha\tau_o+\frac{\beta}{2}\tau_o^2+\frac{\lambda}{3}\tau_o^3\right)}. \tag{3.4}$$

Thus, the conditional posterior distributions π_1^*, π_2^*, and π_3^* for the parameters α, β, and λ are represented as follows:

$$\pi_1^*(\alpha \mid \beta,\lambda,data) \propto \alpha^{\mu_1-1}e^{-\alpha[\nu_1+(n-r_o)\tau_o]}\prod_{i=1}^{r_o}\left(\alpha+\beta y_{i:n}+\lambda y_{i:n}^2\right)e^{-\alpha y_{i:n}}, \tag{3.5}$$

$$\pi_2^*(\beta \mid \alpha,\lambda,data) \propto e^{-\left[\frac{(\beta-\mu_2)^2}{2\nu_2^2}+\beta(n-r_o)\frac{\tau_o^2}{2}\right]}\prod_{i=1}^{r_o}\left(\alpha+\beta y_{i:n}+\lambda y_{i:n}^2\right)e^{-\frac{\beta}{2}y_{i:n}^2}, \tag{3.6}$$

and

$$\pi_3^*(\lambda \mid \alpha,\beta,data) \propto \lambda^{\mu_3-1}e^{-\lambda\left[\nu_3+(n-r_o)\frac{\tau_o^3}{3}\right]}\prod_{i=1}^{r_o}\left(\alpha+\beta y_{i:n}+\lambda y_{i:n}^2\right)e^{-\frac{\lambda}{3}y_{i:n}^3}. \tag{3.7}$$

Bayesian estimates of QHRD parameters are derived using some symmetric (squared error) and asymmetric (linear exponential and general entropy) loss functions:

1. The squared error loss function (SELF) treats deviations from the true parameter equally, regardless of whether they result from overestimation or underestimation, by squaring the difference between the estimate $\hat{\theta}$ and the true value θ as $L(\theta,\hat{\theta}) = (\hat{\theta}-\theta)^2$. Bayesian estimate of any function $g(\alpha,\beta,\lambda)$ is computed under SELF as follows:

$$\hat{g}_{SEL}(\alpha,\beta,\lambda) = E\left[g(\alpha,\beta,\lambda) \mid \text{data}\right] = \int_0^\infty \int_0^\infty \int_{-2\sqrt{\alpha\lambda}}^\infty g(\alpha,\beta,\lambda)\pi^*(\alpha,\beta,\lambda \mid \text{data})\, d\beta\, d\alpha\, d\lambda. \tag{3.8}$$

2. The linear exponential loss function (LINEXLF) differentiates between the costs of overestimation and underestimation by employing a linear exponential form that adjusts sensitivity based on the direction of the error. Proposed by Zellner [50], the LINEXLF is defined by $L(\Delta) = e^{c\Delta} - c\Delta - 1$, where $\Delta = \hat{\theta}-\theta$ and c is a constant that regulates the penalty for deviations. If $c > 0$, overestimations incur greater penalties than underestimations, while if $c < 0$, the reverse holds, with penalties increasing linearly or exponentially based on the value of c. For small values of c, LINEXLF approximates SELF, leading to similar predictions and estimations. However, for larger values of c, the optimal

predictions differ significantly from those derived using SELF. Depending on LINEXLF, the posterior mean for a specific function $g(\alpha,\beta,\lambda)$ serves as the Bayes estimate. This is determined by the following expression:

$$\hat{g}_{LINEX}(\alpha,\beta,\lambda) = \frac{-1}{c}\log\left|E\left[e^{-cg(\alpha,\beta,\lambda)} \mid \text{data}\right]\right| = \frac{-1}{c}\log\left|\int_0^\infty\int_0^\infty\int_{-2\sqrt{\alpha\lambda}}^\infty e^{-c\,g(\alpha,\beta,\lambda)}\pi^*(\alpha,\beta,\lambda \mid \text{data})\,d\beta\,d\alpha\,d\lambda\right|. \tag{3.9}$$

3. General Entropy Loss Function (GELF) represents a significant asymmetric error penalty method that controls sensitivity levels through error magnitude and directions. The GELF presented by Calabria and Pulcini [13] includes the formula $L(\delta) = (\delta)^q - q\log(\delta) - 1$ with $\delta = \frac{\hat{\theta}}{\theta}$ to calculate the penalty strength through the constant q. If $q > 0$, overestimations incur higher penalties than underestimations, and when $q < 0$, the reverse holds. For small values of $|q|$, the GELF approximates the squared-error loss function, providing nearly symmetric penalties when both $\hat{\theta}$ and θ are on a logarithmic scale. An increase in q value leads the loss function to become more asymmetric. Depending on GELF, the posterior mean for a specific function $g(\alpha,\beta,\lambda)$ serves as the Bayes estimate. This is determined by the following expression:

$$\hat{g}_{GEL}(\alpha,\beta,\lambda) = \{E\left[g(\alpha,\beta,\lambda)^{-q} \mid \text{data}\right]\}^{\frac{-1}{q}} = \left\{\int_0^\infty\int_0^\infty\int_{-2\sqrt{\alpha\lambda}}^\infty g(\alpha,\beta,\lambda)^{-q}\pi^*(\alpha,\beta,\lambda \mid \text{data})\,d\beta\,d\alpha\,d\lambda\right\}^{\frac{-1}{q}}, \tag{3.10}$$

which minimizes the expected loss. Furthermore, when $q = 1$, the GELF coincides with the weighted SELF, while when $q = -1$, the GELF coincides with the SELF, which reflects the flexibility of the Entropy Loss in accommodating different types of estimation errors depending on the context.

Due to the complexity of the multivariate integrals involved, as shown in Equations (3.8), (3.9), and (3.10). Obtaining Bayesian estimates for the parameters α, β, and λ, along with their highest posterior density (HPD) credible intervals, poses considerable challenges. As a result, approximate approaches such as Markov Chain Monte Carlo (MCMC) are employed to generate samples from the posterior distributions given by $\pi^*(\alpha,\beta,\lambda \mid \text{data})$.

Gibbs sampling is commonly employed for this purpose. However, the conditional distributions π_1^*, π_2^*, and π_3^* in Equations (3.5), (3.6), and (3.7) do not follow standard distributions, rendering Gibbs sampling insufficient on its own. For that, integrate the Metropolis-Hastings (M-H) algorithm into the MCMC process. This approach is particularly effective due to the strong similarity between the conditional distributions, represented by π_1^*, π_2^*, and π_3^*, which closely resemble normal distributions, as shown in Figure 2.

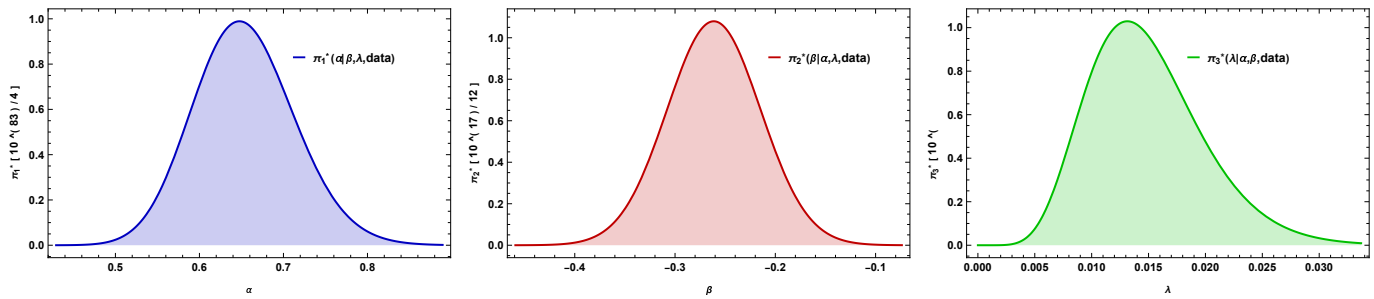

Figure 2. Conditional posterior densities for α **(left)**, β **(center)**, and λ **(right)**.

The M-H algorithm generates proposals using normal distributions because MCMC methods require

symmetric proposal distributions. The acceptance function within the M-H framework ensures that the resulting distribution conforms to the target posterior distribution; see Lynch [36].

3.1. Metropolis-Hasting Algorithm

The procedure of the M-H algorithm as part of Gibbs sampling, as illustrated by Tierney [47] and elaborated by Gilks et al. [25], is implemented as follows:

1. Initialize the parameter values as $\theta_i^{(0)} = \hat{\theta}_{i_{ML}}$ for $i = 1, 2, 3$, where $\theta_1 = \alpha$, $\theta_2 = \beta$, and $\theta_3 = \lambda$.
2. Put $j = 1$ to start the iteration.
3. The proposals $\theta_i^{(j)}$ for $i = 1, 2, 3$ are generated from the conditional distributions:

$$\pi_1^*\left(\theta_1^{(j-1)} \mid \theta_2^{(j-1)}, \theta_3^{(j-1)}, \text{data}\right), \quad \pi_2^*\left(\theta_2^{(j-1)} \mid \theta_1^{(j)}, \theta_3^{(j-1)}, \text{data}\right), \quad \text{and} \quad \pi_3^*\left(\theta_3^{(j-1)} \mid \theta_1^{(j)}, \theta_2^{(j)}, \text{data}\right),$$

   where each proposal is drawn from a normal distribution $N\left(\theta_i^{(j-1)}, \hat{\sigma}^2_{\hat{\theta}_i}\right)$ for $i = 1, 2, 3$. This process is executed using the M-H algorithm as outlined below. The variance $\hat{\sigma}^2_{\hat{\theta}_i}$ is determined from the principal diagonal of the inverse FIM.

   (i) The proposals θ_i^* for $i = 1, 2, 3$ are generated from $N\left(\theta_i^{(j-1)}, \hat{\sigma}^2_{\hat{\theta}_i}\right)$.

   (ii) Assessing the acceptance probabilities using the following equations:

$$\left.\begin{aligned} \eta_{\theta_1} &= \min\left[1, \frac{\pi_1^*\left(\theta_1^* \mid \theta_2^{(j-1)}, \theta_3^{(j-1)}, \text{data}\right)}{\pi_1^*\left(\theta_1^{(j-1)} \mid \theta_2^{(j-1)}, \theta_3^{(j-1)}, \text{data}\right)}\right], \\ \eta_{\theta_2} &= \min\left[1, \frac{\pi_2^*\left(\theta_2^* \mid \theta_1^{(j)}, \theta_3^{(j-1)}, \text{data}\right)}{\pi_2^*\left(\theta_2^{(j-1)} \mid \theta_1^{(j)}, \theta_3^{(j-1)}, \text{data}\right)}\right], \text{ and} \\ \eta_{\theta_3} &= \min\left[1, \frac{\pi_3^*\left(\theta_3^* \mid \theta_1^{(j)}, \theta_2^{(j)}, \text{data}\right)}{\pi_3^*\left(\theta_3^{(j-1)} \mid \theta_1^{(j)}, \theta_2^{(j)}, \text{data}\right)}\right]. \end{aligned}\right\}$$

   (iii) Generate u_i for $i = 1, 2, 3$ from the uniform distribution $U(0, 1)$.

   (iv) If $u_i < \eta_{\theta_i}$ is satisfied for $i = 1, 2, 3$, accept the proposal and put $\theta_i^{(j)} = \theta_i^*$. Else, $\theta_i^{(j)} = \theta_i^{(j-1)}$.

4. Compute $\theta_i^{(j)}$ for $i = 1, 2, 3$.
5. Compute $S(t) = \theta_4$ and $h(t) = \theta_5$ as follows:

$$S(t)^{(j)} = e^{-\left(\theta_1^{(j)} t + \frac{\theta_2^{(j)}}{2} t^2 + \frac{\theta_3^{(j)}}{3} t^3\right)} \quad \text{and} \quad h(t)^{(j)} = \left(\theta_1^{(j)} + \theta_2^{(j)} t + \theta_3^{(j)} t^2\right).$$

6. Update j to $j + 1$.
7. Reiterate steps (**3**) through (**6**) for $\mathcal{N}$ times to get $\theta_i^{(j)}$ for $i = 1, 2, 3, 4, 5$ and $j = 1, 2, \ldots, \mathcal{N}$.

The first $\mathcal{M}$ samples generated will be discarded as burn-in to ensure convergence and mitigate the effect of start values. Consequently, with a sufficiently large number of samples $\mathcal{N}$, the remaining samples $\theta_i^{(j)}$ for $i = 1, 2, 3, 4, 5$ provide approximate posterior samples, which are used to refine Bayesian estimates. Specifically, using the MCMC simulated values $\theta_i^{(j)}$ for $j = \mathcal{M} + 1, \mathcal{M} + 2, \ldots, \mathcal{N}$, the Bayesian estimates $\hat{\theta}_{i_{BS}}$ are computed under SELF, LINEXLF, and GELF as follows:

$$\hat{\theta}_{i_{SEL}} = \frac{1}{\mathcal{N} - \mathcal{M}} \sum_{j=\mathcal{M}+1}^{\mathcal{N}} \theta_i^{(j)}, \; \hat{\theta}_{i_{LINEX}} = \frac{-1}{c} \log\left[\frac{1}{\mathcal{N} - \mathcal{M}} \sum_{j=\mathcal{M}+1}^{\mathcal{N}} e^{-c(\theta_i^{(j)})}\right], \text{ and } \hat{\theta}_{i_{GEL}} = \left\{\frac{1}{\mathcal{N} - \mathcal{M}} \sum_{j=\mathcal{M}+1}^{\mathcal{N}} (\theta_i^{(j)})^{-q}\right\}^{\frac{-1}{q}}.$$

To calculate the HPD credible intervals for θ_i where $i = 1, 2, 3, 4, 5$, follow these steps:

1. Arrange the generated values $\theta_i^{(j)}$ as:

$$\theta_i^{(\mathcal{M}+1)} < \theta_i^{(\mathcal{M}+2)} < \theta_i^{(\mathcal{M}+3)} < \ldots < \theta_i^{(\mathcal{N})}.$$

2. Determine the $100(1-\gamma)\%$ HPD credible intervals for each θ_i using the formula:

$$(\theta_{i_L}, \theta_{i_U}) = \left(\theta_i^{(j^*)}, \theta_i^{(j^*+\lfloor(1-\gamma)(\mathcal{N}-\mathcal{M})\rfloor)}\right),$$

where θ_{i_L} and θ_{i_U} are their lower and upper bounds, and $j^* = \mathcal{M}+1, \mathcal{M}+2, \ldots, \mathcal{N}$ is given by:

$$\theta_i^{(j^*+\lfloor(1-\gamma)(\mathcal{N}-\mathcal{M})\rfloor)} - \theta_i^{(j^*)} = \min_{1\le j\le\gamma(\mathcal{N}-\mathcal{M})}\left(\theta_i^{(j+\lfloor(1-\gamma)(\mathcal{N}-\mathcal{M})\rfloor)} - \theta_i^{(j)}\right),$$

where $\lfloor\chi\rfloor$ represents the largest integer $\le \chi$.

3.2. Hyperparameters Selection

Bayesian analysis requires appropriate hyperparameter value selection when employing informative priors. The determination of these values involves a combination of expert knowledge, prior studies, or empirical data to ensure a meaningful representation of prior beliefs about the parameters. This approach enhances both the reliability and interpretability of the model; see Jaheen [30], Dey et al. [15], and Singh and Tripathi [44]. Let O denote the total number of complete random samples generated from the QHRD. For each sample i, where $i = 1, 2, \ldots, O$, let $(\hat{\alpha}_i, \hat{\beta}_i, \hat{\lambda}_i)$ represent the MLEs of (α, β, λ). Then the hyperparameter values are selected by equating the mean and variance of $(\hat{\alpha}_i, \hat{\beta}_i, \hat{\lambda}_i)$ with the corresponding average and variance of the predefined priors. In this study, the prior distributions of (α, β, λ) are defined in Equation (3.1), where their averages and variances are as follows:

$$\bar{\alpha} = \frac{\mu_1}{\nu_1}, \quad \mathrm{Var}(\alpha) = \frac{\mu_1}{\nu_1^2}, \quad \bar{\beta} = \mu_2, \quad \mathrm{Var}(\beta) = \nu_2^2, \quad \bar{\lambda} = \frac{\mu_3}{\nu_3}, \quad \text{and} \quad \mathrm{Var}(\lambda) = \frac{\mu_3}{\nu_3^2}.$$

Consequently, matching the average and variance values of $(\hat{\alpha}_i, \hat{\beta}_i, \hat{\lambda}_i)$ for $i = 1, 2, \ldots, O$ with their correspondence in the previous identities yields

$$\frac{1}{O}\sum_{i=1}^{O}\hat{\alpha}_i = \frac{\mu_1}{\nu_1} \quad \text{and} \quad \frac{1}{O-1}\sum_{i=1}^{O}(\hat{\alpha}_i - \frac{1}{O}\sum_{i=1}^{O}\hat{\alpha}_i)^2 = \frac{\mu_1}{\nu_1^2}.$$

$$\frac{1}{O}\sum_{i=1}^{O}\hat{\beta}_i = \mu_2 \quad \text{and} \quad \frac{1}{O-1}\sum_{i=1}^{O}(\hat{\beta}_i - \frac{1}{O}\sum_{i=1}^{O}\hat{\beta}_i)^2 = \nu_2^2.$$

$$\frac{1}{O}\sum_{i=1}^{O}\hat{\lambda}_i = \frac{\mu_3}{\nu_3} \quad \text{and} \quad \frac{1}{O-1}\sum_{i=1}^{O}(\hat{\lambda}_i - \frac{1}{O}\sum_{i=1}^{O}\hat{\lambda}_i)^2 = \frac{\mu_3}{\nu_3^2}.$$

The estimates of the hyperparameters μ_1, ν_1, μ_2, ν_2, μ_3, and ν_3 are given by solving the above three equations simultaneously and expressing the results in the following manner:

$$\hat{\mu}_1 = \frac{(\frac{1}{O}\sum_{i=1}^{O}\hat{\alpha}_i)^2}{\frac{1}{O-1}\sum_{i=1}^{O}(\hat{\alpha}_i - \frac{1}{O}\sum_{i=1}^{O}\hat{\alpha}_i)^2} \quad \text{and} \quad \hat{\nu}_1 = \frac{\frac{1}{O}\sum_{i=1}^{O}\hat{\alpha}_i}{\frac{1}{O-1}\sum_{i=1}^{O}(\hat{\alpha}_i - \frac{1}{O}\sum_{i=1}^{O}\hat{\alpha}_i)^2}.$$

$$\hat{\mu}_2 = \frac{1}{O}\sum_{i=1}^{O}\hat{\beta}_i \quad \text{and} \quad \hat{v}_2^2 = \frac{1}{O-1}\sum_{i=1}^{O}(\hat{\beta}_i - \frac{1}{O}\sum_{i=1}^{O}\hat{\beta}_i)^2.$$

$$\hat{\mu}_3 = \frac{(\frac{1}{O}\sum_{i=1}^{O}\hat{\lambda}_i)^2}{\frac{1}{O-1}\sum_{i=1}^{O}(\hat{\lambda}_i - \frac{1}{O}\sum_{i=1}^{O}\hat{\lambda}_i)^2} \quad \text{and} \quad \hat{v}_3 = \frac{\frac{1}{O}\sum_{i=1}^{O}\hat{\lambda}_i}{\frac{1}{O-1}\sum_{i=1}^{O}(\hat{\lambda}_i - \frac{1}{O}\sum_{i=1}^{O}\hat{\lambda}_i)^2}.$$

4. Simulation Study

The simulation analysis evaluates the performance and accuracy of both point and interval estimators using ML and their Bayesian counterparts for parameters α, β, and λ, as well as $S(t)$ and $h(t)$. A total of $\mathcal{B} = 1,000$ H-T-II censored samples were generated from the QHRD for each simulation using the Wolfram Mathematica 13.1 program. The initial parameter values were set as follows: $\alpha_0 = 0.656$, $\beta_0 = -0.164$, and $\lambda_0 = 0.015$. At $t = 0.15$, $S(t = 0.15) = 0.908$ and $h(t = 0.15) = 0.632$. The study investigates various combinations of sample size n together with a predetermined failure count r and a predetermined time τ. Specifically, we examine the following scenarios: $(n, r, \tau) = (30, 18, 2)$, $(30, 18, 3)$, $(30, 18, 4)$, $(30, 23, 2)$, $(30, 23, 3)$, $(30, 23, 4)$, $(60, 35, 2)$, $(60, 35, 3)$, $(60, 35, 4)$, $(60, 45, 2)$, $(60, 45, 3)$, $(60, 45, 4)$, $(90, 50, 2)$, $(90, 50, 3)$, $(90, 50, 4)$, $(90, 65, 2)$, $(90, 65, 3)$, and $(90, 65, 4)$. The estimation process is carried out in several main steps:

1. Define the sample size n, the predetermined number of failures r, and the predetermined time τ. Set the initial values for the parameters α, β, and λ as α_0, β_0, and λ_0, respectively.
2. Generate independent random samples of size n from the QHRD and sort them as $y_{i:n}$ for $i = 1, 2, \ldots, n$ using the initial parameter values. This process employs $F(y_{i:n}; \alpha, \beta, \lambda)$ as defined in Equation (1.3).
3. Extract the H-T-II censored sample by recording observations up to time $\max(y_{r:n}, \tau)$, making sure to observe exactly r_o of failure.
4. After obtaining the required H-II-T censored sample through steps $(1 - 3)$, compute the MLEs for α, β, and λ, along with $S(t)$ and $h(t)$. Then construct their corresponding 95% ACIs.
5. To estimate α, β, λ, $S(t)$, and $h(t)$ using Bayesian inference, first define the hyperparameters for informative priors, as described in subsection 3.2. Generate $O = 500$ complete random samples, each containing 100 observations, from the QHRD using historical data with varying parameter values. Implement the MCMC algorithm, running it for $\mathcal{N} = 12,000$ iterations while discarding the first $\mathcal{M} = 2,000$ samples as burn-in. Then construct their corresponding 95% HPD credible intervals.
6. Repeat steps $(1 - 5)$ for a total of $\mathcal{B} = 1,000$ iterations.
7. Compute the average estimates (AEsts) for the MLEs and BEs under different loss functions using the following formula:

$$\text{AEst}(\theta_i) = \frac{1}{\mathcal{B}}\sum_{j=1}^{\mathcal{B}}\hat{\theta}_i^{(j)}.$$

For the accuracy and robustness of point estimates, use the root mean square error (RMSE) and mean absolute relative bias (MRAB) criteria:

$$\text{RMSE}(\theta_i) = \sqrt{\frac{1}{\mathcal{B}}\sum_{j=1}^{\mathcal{B}}\left(\hat{\theta}_i^{(j)} - \theta_i\right)^2} \quad \text{and} \quad \text{MRAB}(\theta_i) = \frac{1}{\mathcal{B}}\sum_{j=1}^{\mathcal{B}}\left|\frac{\hat{\theta}_i^{(j)} - \theta_i}{\theta_i}\right|.$$

On the other hand, for the accuracy and robustness of interval estimates, use the criteria of average confidence interval length (AL) and coverage probability (CP):

$$\mathrm{AL}_{(1-\gamma)\%}(\theta_i) = \frac{1}{\mathcal{B}}\sum_{j=1}^{\mathcal{B}}\left(\hat{\theta}_{i_U} - \hat{\theta}_{i_L}\right) \quad \text{and} \quad \mathrm{CP}_{(1-\gamma)\%}(\theta_i) = \frac{1}{\mathcal{B}}\sum_{j=1}^{\mathcal{B}}\mathbf{1}_{(\hat{\theta}_{i_L};\hat{\theta}_{i_U})}(\theta_i).$$

The findings for AEst, RMSE, MRAB, 95% AL, and 95% CP concerning each parameter within the H-T-II CS framework are presented in Tables 1, 2, 3, 4, 5, and 6. Several insights into the performance of point and interval estimates can be provided, specifically in relation to decreasing RMSE, MRAB, and AL while increasing CP. Notably, it is evident that:

1. Overall, BEs demonstrate lower RMSE and MRAB values, narrower ALs, and higher CPs compared to MLEs, indicating that BEs outperform MLEs in these respects.
2. For fixed values of n and r, increasing τ generally leads to decreasing RMSE and MRAB and ALs while the CPs increase for all estimators in most cases.
3. For fixed values of n and τ, increasing r generally leads to higher RMSE and lower MRAB, ALs, and CPs for the parameters α and $S(t)$. Similarly, for β, RMSE and MRAB increase, while ALs and CPs decrease. In contrast, for λ and $h(t)$, increases in r result in decreases in RMSE, MRAB, ALs, and CPs.
4. In summary, we recommend the use of the Bayesian approach and the MCMC method for estimating the unknown parameters, as well as $S(t)$ and $h(t)$ of the QHRD based on H-T-II CS.

5. Real Data Applications

This section provides applications of estimation methods for demonstrating the practical utility and effectiveness of the QHRD within the H-T-II CS framework. In this case, we are concerned with two real-life medical datasets that detail COVID-19 mortality rates from different regions. Firstly, we focus on the dataset analyzed by Alghamdi and Abd El-Raouf [2], which covers COVID-19 mortality rates in the United Kingdom over 76 days from April 15 to June 30, 2020. Secondly, we analyze COVID-19 mortality rates in Albania over 104 days, from April 19 to July 31, 2020. Both datasets are publicly available on the WHO website [https://covid19.who.int/]. Details of these datasets are provided in ascending order below in Tables 7 and 8.

Before proceeding, we first estimate the parameters of the QHRD along with their standard error (St.Er). Next, we perform goodness-of-fit tests, including the Cramér-von Mises (W^*), Anderson-Darling (A^*), and Kolmogorov-Smirnov ($K-S$) tests with the $K-S$ connected P-value and some information measures, including the -2log-likelihood (-2ℓ), Akaike Information Criterion (AIC), Consistent Akaike Information Criterion (CAIC), Bayesian Information Criterion (BIC), and Hannan-Quinn Information Criterion (HQIC) to evaluate the adequacy of the QHRD and its CDF fit to the dataset. We also compare the performance of the QHRD with several competing distributions, specifically the Log-Logistic distribution (LLD) from Singh [45], the Inverted Exponentiated Lomax Distribution (IELD) proposed by Elmorsy and Hassan [23], the Weibull-Gamma Distribution (WGD) introduced by Nadarajah and Kotz [40], the Lomax Distribution (LOD), the Alpha Power Inverse Weibull Distribution (APIWD) introduced by [11], the Weibull distribution (WD) from Weibull [48], the Linear Hazard Rate distribution (LHRD) proposed by Bain [9], the Power

Table 1. Results of the point estimate for α under H-T-II CS.

						LINEXLF			GELF	
n	r	τ		MLE	SELF	$c = -3$	$c = 0.0001$	$c = 3$	$q = -1$	$q = 1$
			AEst	0.80783	0.64692	0.65512	0.64692	0.63900	0.64692	0.63866
30	18	2	RMSE	0.32848	0.04326	0.04335	0.04326	0.04468	0.04326	0.04525
			MRAB	0.38689	0.05280	0.05235	0.05280	0.05540	0.05280	0.05614
			AEst	0.77954	0.65287	0.66063	0.65287	0.64535	0.65287	0.64509
30	18	3	RMSE	0.25809	0.04289	0.04397	0.04289	0.04320	0.04289	0.04372
			MRAB	0.30927	0.05235	0.05405	0.05235	0.05196	0.05235	0.05258
			AEst	0.74519	0.65038	0.65776	0.65038	0.64321	0.65038	0.64295
30	18	4	RMSE	0.22743	0.04050	0.04102	0.04050	0.04129	0.04050	0.04177
			MRAB	0.25152	0.04935	0.04871	0.04935	0.05119	0.04935	0.05181
			AEst	0.78514	0.65022	0.65782	0.65022	0.64284	0.65022	0.64258
30	23	2	RMSE	0.27277	0.04170	0.04255	0.04170	0.04224	0.04170	0.04275
			MRAB	0.31547	0.05123	0.05154	0.05123	0.05218	0.05123	0.05281
			AEst	0.81902	0.65559	0.66325	0.65559	0.64813	0.65559	0.64791
30	23	3	RMSE	0.29739	0.03403	0.03572	0.03403	0.03402	0.03403	0.03442
			MRAB	0.33324	0.04169	0.04311	0.04169	0.04258	0.04169	0.04310
			AEst	0.73826	0.64546	0.65271	0.64546	0.63841	0.64546	0.63810
30	23	4	RMSE	0.20908	0.03452	0.03381	0.03452	0.03662	0.03452	0.03707
			MRAB	0.25698	0.04253	0.04072	0.04253	0.04606	0.04253	0.04666
			AEst	0.80715	0.64830	0.65462	0.64830	0.64215	0.64830	0.64191
60	35	2	RMSE	0.24484	0.04466	0.04472	0.04466	0.04547	0.04466	0.04593
			MRAB	0.29040	0.05663	0.05636	0.05663	0.05771	0.05663	0.05828
			AEst	0.75386	0.64589	0.65154	0.64589	0.64038	0.64589	0.64015
60	35	3	RMSE	0.17454	0.04165	0.04121	0.04165	0.04282	0.04165	0.04322
			MRAB	0.20769	0.05062	0.04903	0.05062	0.05312	0.05062	0.05364
			AEst	0.72880	0.65798	0.66347	0.65798	0.65262	0.65798	0.65250
60	35	4	RMSE	0.16814	0.03707	0.03829	0.03707	0.03666	0.03707	0.03696
			MRAB	0.20000	0.04448	0.04522	0.04448	0.04469	0.04448	0.04507
			AEst	0.75763	0.65309	0.65889	0.65309	0.64744	0.65309	0.64729
60	45	2	RMSE	0.18344	0.03811	0.03897	0.03811	0.03813	0.03811	0.03849
			MRAB	0.21564	0.04697	0.04647	0.04697	0.04813	0.04697	0.04859
			AEst	0.75463	0.65156	0.65723	0.65156	0.64604	0.65156	0.64587
60	45	3	RMSE	0.18694	0.03954	0.03999	0.03954	0.03989	0.03954	0.04025
			MRAB	0.21866	0.04810	0.04761	0.04810	0.04945	0.04810	0.04991
			AEst	0.72893	0.64453	0.65008	0.64453	0.63912	0.64453	0.63890
60	45	4	RMSE	0.18475	0.04035	0.03984	0.04035	0.04158	0.04035	0.04196
			MRAB	0.21404	0.05268	0.05107	0.05268	0.05505	0.05268	0.05556
			AEst	0.73934	0.64226	0.64730	0.64226	0.63733	0.64226	0.63710
90	50	2	RMSE	0.17536	0.04428	0.04350	0.04428	0.04559	0.04428	0.04597
			MRAB	0.20018	0.05818	0.05716	0.05818	0.05961	0.05818	0.06010
			AEst	0.73854	0.65609	0.66068	0.65609	0.65158	0.65609	0.65148
90	50	3	RMSE	0.16949	0.04452	0.04525	0.04452	0.04425	0.04452	0.04456
			MRAB	0.20064	0.05466	0.05503	0.05466	0.05509	0.05466	0.05550
			AEst	0.72703	0.66299	0.66751	0.66299	0.65857	0.66299	0.65852
90	50	4	RMSE	0.15240	0.04191	0.04331	0.04191	0.04099	0.04191	0.04126
			MRAB	0.18561	0.05214	0.05436	0.05214	0.05056	0.05214	0.05089
			AEst	0.74725	0.65904	0.66390	0.65904	0.65428	0.65904	0.65420
90	65	2	RMSE	0.17371	0.03754	0.03889	0.03754	0.03682	0.03754	0.03708
			MRAB	0.20658	0.04694	0.04829	0.04694	0.04625	0.04694	0.04659
			AEst	0.72543	0.64713	0.65167	0.64713	0.64269	0.64713	0.64253
90	65	3	RMSE	0.16870	0.03902	0.03875	0.03902	0.03980	0.03902	0.04009
			MRAB	0.18812	0.04950	0.04905	0.04950	0.05050	0.04950	0.05087
			AEst	0.73391	0.67064	0.67521	0.67064	0.66617	0.67064	0.66617
90	65	4	RMSE	0.15471	0.03995	0.04223	0.03995	0.03812	0.03995	0.03837
			MRAB	0.18845	0.04678	0.04940	0.04678	0.04484	0.04678	0.04512

Table 2. Results of the point estimate for β under H-T-II CS.

						LINEXLF			GELF	
n	r	τ		MLE	SELF	$c = -3$	$c = 0.0001$	$c = 3$	$q = -1$	$q = 1$
			AEst	−0.77823	−0.17532	−0.17326	−0.17532	−0.17735	−0.17532	−0.16567
30	18	2	RMSE	0.79825	0.01237	0.01061	0.01237	0.01421	0.01237	0.00683
			MRAB	3.82796	0.06900	0.05663	0.06900	0.08142	0.06900	0.02954
			AEst	−0.50529	−0.18141	−0.17950	−0.18141	−0.18330	−0.18141	−0.17344
30	18	3	RMSE	0.48187	0.01801	0.01622	0.01801	0.01982	0.01801	0.01105
			MRAB	2.15354	0.10613	0.09453	0.10613	0.11769	0.10613	0.06097
			AEst	−0.34135	−0.18998	−0.18830	−0.18998	−0.19167	−0.18998	−0.18360
30	18	4	RMSE	0.26666	0.02660	0.02499	0.02660	0.02822	0.02660	0.02066
			MRAB	1.18751	0.15843	0.14818	0.15843	0.16869	0.15843	0.11951
			AEst	−0.52253	−0.18642	−0.18461	−0.18642	−0.18822	−0.18642	−0.17898
30	23	2	RMSE	0.51316	0.02542	0.02400	0.02542	0.02690	0.02542	0.02060
			MRAB	2.27835	0.13703	0.12630	0.13703	0.14772	0.13703	0.10073
			AEst	−0.52843	−0.18554	−0.18372	−0.18554	−0.18734	−0.18554	−0.17820
30	23	3	RMSE	0.51166	0.02326	0.02170	0.02326	0.02485	0.02326	0.01760
			MRAB	2.30812	0.13131	0.12027	0.13131	0.14232	0.13131	0.08770
			AEst	−0.37488	−0.19071	−0.18905	−0.19071	−0.19237	−0.19071	−0.18432
30	23	4	RMSE	0.29813	0.02780	0.02626	0.02780	0.02935	0.02780	0.02221
			MRAB	1.40338	0.16284	0.15272	0.16284	0.17297	0.16284	0.12387
			AEst	−0.64216	−0.18952	−0.18763	−0.18952	−0.19140	−0.18952	−0.18209
60	35	2	RMSE	0.60280	0.02585	0.02400	0.02585	0.02769	0.02585	0.01870
			MRAB	2.96076	0.15561	0.14411	0.15561	0.16705	0.15561	0.11028
			AEst	−0.40754	−0.20443	−0.20281	−0.20443	−0.20606	−0.20443	−0.19883
60	35	3	RMSE	0.31999	0.04072	0.03912	0.04072	0.04232	0.04072	0.03523
			MRAB	1.54056	0.24655	0.23667	0.24655	0.25647	0.24655	0.21241
			AEst	−0.29730	−0.21569	−0.21420	−0.21569	−0.21717	−0.21569	−0.21090
60	35	4	RMSE	0.20883	0.05204	0.05058	0.05204	0.05351	0.05204	0.04735
			MRAB	0.98270	0.31515	0.30612	0.31515	0.32421	0.31515	0.28598
			AEst	−0.44014	−0.20468	−0.20302	−0.20468	−0.20633	−0.20468	−0.19880
60	45	2	RMSE	0.38884	0.04243	0.04092	0.04243	0.04395	0.04243	0.03733
			MRAB	1.72245	0.24802	0.23794	0.24802	0.25811	0.24802	0.21222
			AEst	−0.38975	−0.20815	−0.20656	−0.20815	−0.20974	−0.20815	−0.20275
60	45	3	RMSE	0.30608	0.04503	0.04351	0.04503	0.04656	0.04503	0.03995
			MRAB	1.46008	0.26920	0.25952	0.26920	0.27889	0.26920	0.23630
			AEst	−0.36123	−0.20959	−0.20804	−0.20959	−0.21115	−0.20959	−0.20437
60	45	4	RMSE	0.27015	0.04659	0.04511	0.04659	0.04808	0.04659	0.04170
			MRAB	1.27652	0.27800	0.26853	0.27800	0.28750	0.27800	0.24617
			AEst	−0.46915	−0.20153	−0.19980	−0.20153	−0.20326	−0.20153	−0.19539
90	50	2	RMSE	0.41475	0.03765	0.03593	0.03765	0.03937	0.03765	0.03156
			MRAB	1.89596	0.22882	0.21826	0.22882	0.23938	0.22882	0.19141
			AEst	−0.37132	−0.22244	−0.22088	−0.22244	−0.22401	−0.22244	−0.21754
90	50	3	RMSE	0.28219	0.05865	0.05710	0.05865	0.06021	0.05865	0.05380
			MRAB	1.38916	0.35635	0.34681	0.35635	0.36591	0.35635	0.32647
			AEst	−0.29114	−0.23672	−0.23533	−0.23672	−0.23812	−0.23672	−0.23268
90	50	4	RMSE	0.18902	0.07291	0.07153	0.07292	0.07431	0.07291	0.06890
			MRAB	0.90135	0.44343	0.43493	0.44343	0.45197	0.44343	0.41880
			AEst	−0.40953	−0.21596	−0.21434	−0.21596	−0.21759	−0.21596	−0.21058
90	65	2	RMSE	0.34254	0.05361	0.05208	0.05361	0.05514	0.05361	0.04870
			MRAB	1.57154	0.31685	0.30693	0.31685	0.32678	0.31685	0.28405
			AEst	−0.33933	−0.22640	−0.22489	−0.22640	−0.22791	−0.22640	−0.22178
90	65	3	RMSE	0.27557	0.06276	0.06127	0.06276	0.06426	0.06276	0.05822
			MRAB	1.13968	0.38046	0.37127	0.38046	0.38968	0.38046	0.35229
			AEst	−0.28733	−0.23671	−0.23531	−0.23671	−0.23811	−0.23671	−0.23264
90	65	4	RMSE	0.17734	0.07294	0.07155	0.07294	0.07433	0.07294	0.06890
			MRAB	0.87950	0.44332	0.43480	0.44332	0.45188	0.44332	0.41853

Table 3. Results of the point estimate for λ under H-T-II CS.

						LINEXLF			GELF	
n	r	τ		MLE	SELF	$c = -3$	$c = 0.0001$	$c = 3$	$q = -1$	$q = 1$
			AEst	0.35717	0.01954	0.01959	0.01954	0.01949	0.01954	0.01798
30	18	2	RMSE	0.42633	0.00457	0.00461	0.00457	0.00452	0.00457	0.00303
			MRAB	22.8111	0.30261	0.30567	0.30261	0.29957	0.30261	0.19865
			AEst	0.15948	0.01938	0.01943	0.01938	0.01934	0.01938	0.01787
30	18	3	RMSE	0.19179	0.00443	0.00447	0.00443	0.00438	0.00443	0.00293
			MRAB	9.64898	0.29207	0.29502	0.29207	0.28914	0.29207	0.19106
			AEst	0.06961	0.01931	0.01935	0.01931	0.01927	0.01931	0.01789
30	18	4	RMSE	0.07513	0.00439	0.00443	0.00439	0.00435	0.00439	0.00301
			MRAB	3.66091	0.28740	0.29014	0.28740	0.28468	0.28740	0.19255
			AEst	0.17585	0.01947	0.01951	0.01947	0.01943	0.01947	0.01803
30	23	2	RMSE	0.24051	0.00452	0.00456	0.00452	0.00448	0.00452	0.00312
			MRAB	10.7752	0.29795	0.30075	0.29795	0.29517	0.29795	0.20184
			AEst	0.15312	0.01937	0.01941	0.01937	0.01933	0.01937	0.01792
30	23	3	RMSE	0.18631	0.00440	0.00444	0.00440	0.00436	0.00440	0.00298
			MRAB	9.22423	0.29113	0.29393	0.29113	0.28834	0.29113	0.19437
			AEst	0.08246	0.01932	0.01936	0.01932	0.01928	0.01932	0.01794
30	23	4	RMSE	0.08808	0.00437	0.00441	0.00437	0.00434	0.00437	0.00303
			MRAB	4.51974	0.28810	0.29076	0.28810	0.28545	0.28810	0.19570
			AEst	0.26171	0.02041	0.02046	0.02041	0.02036	0.02041	0.01890
60	35	2	RMSE	0.30754	0.00546	0.00551	0.00546	0.00541	0.00546	0.00397
			MRAB	16.4594	0.36060	0.36369	0.36060	0.35753	0.36060	0.25975
			AEst	0.10599	0.02105	0.02109	0.02105	0.02100	0.02105	0.01964
60	35	3	RMSE	0.11319	0.00614	0.00618	0.00614	0.00610	0.00614	0.00476
			MRAB	6.08803	0.40310	0.40605	0.40310	0.40018	0.40310	0.30928
			AEst	0.05546	0.02142	0.02146	0.02142	0.02138	0.02142	0.02018
60	35	4	RMSE	0.05572	0.00654	0.00658	0.00654	0.00650	0.00654	0.00534
			MRAB	2.75249	0.42782	0.43041	0.42782	0.42524	0.42782	0.34557
			AEst	0.14342	0.02107	0.02112	0.02107	0.02103	0.02107	0.01971
60	45	2	RMSE	0.19141	0.00620	0.00625	0.00620	0.00616	0.00620	0.00491
			MRAB	8.57325	0.40494	0.40778	0.40494	0.40212	0.40494	0.31404
			AEst	0.09750	0.02119	0.02123	0.02119	0.02115	0.02119	0.01985
60	45	3	RMSE	0.10749	0.00631	0.00635	0.00631	0.00627	0.00631	0.00503
			MRAB	5.52627	0.41259	0.41540	0.41259	0.40980	0.41259	0.32331
			AEst	0.08601	0.02137	0.02141	0.02137	0.02133	0.02137	0.02005
60	45	4	RMSE	0.09060	0.00650	0.00654	0.00650	0.00646	0.00650	0.00525
			MRAB	4.75470	0.42475	0.42753	0.42475	0.42200	0.42475	0.33698
			AEst	0.17684	0.02139	0.02144	0.02139	0.02134	0.02139	0.01992
90	50	2	RMSE	0.20744	0.00644	0.00648	0.00644	0.00639	0.00644	0.00498
			MRAB	10.7945	0.42589	0.42904	0.42589	0.42275	0.42589	0.32779
			AEst	0.09657	0.02285	0.02289	0.02285	0.02280	0.02285	0.02151
90	50	3	RMSE	0.10030	0.00797	0.00802	0.00797	0.00793	0.00797	0.00666
			MRAB	5.46312	0.52313	0.52612	0.52313	0.52015	0.52313	0.43400
			AEst	0.05062	0.02394	0.02398	0.02394	0.02390	0.02394	0.02283
90	50	4	RMSE	0.04867	0.00906	0.00910	0.00906	0.00902	0.00906	0.00796
			MRAB	2.49495	0.59614	0.59876	0.59614	0.59353	0.59614	0.52189
			AEst	0.13353	0.02237	0.02242	0.02237	0.02233	0.02237	0.02102
90	65	2	RMSE	0.15621	0.00762	0.00766	0.00762	0.00758	0.00762	0.00635
			MRAB	7.91407	0.49163	0.49461	0.49163	0.48867	0.49163	0.40128
			AEst	0.07611	0.02348	0.02352	0.02348	0.02343	0.02348	0.02220
90	65	3	RMSE	0.09300	0.00860	0.00865	0.00860	0.00856	0.00860	0.00736
			MRAB	4.09927	0.56516	0.56811	0.56516	0.56223	0.56516	0.47984
			AEst	0.05001	0.02373	0.02377	0.02373	0.02369	0.02373	0.02262
90	65	4	RMSE	0.04616	0.00883	0.00887	0.00883	0.00879	0.00883	0.00774
			MRAB	2.41508	0.58215	0.58473	0.58215	0.57958	0.58215	0.50818

Table 4. Results of the point estimate for $S(t = 0.15)$ under H-T-II CS.

						LINEXLF			GELF	
n	r	τ		MLE	SELF	$c = -3$	$c = 0.0001$	$c = 3$	$q = -1$	$q = 1$
			AEst	0.89399	0.90937	0.90951	0.90937	0.90922	0.90937	0.90926
30	18	2	RMSE	0.03725	0.00597	0.00599	0.00597	0.00595	0.00597	0.00595
			MRAB	0.03212	0.00527	0.00530	0.00527	0.00524	0.00527	0.00525
			AEst	0.89499	0.90861	0.90875	0.90861	0.90848	0.90861	0.90851
30	18	3	RMSE	0.03050	0.00589	0.00589	0.00589	0.00589	0.00589	0.00589
			MRAB	0.02687	0.00517	0.00517	0.00517	0.00518	0.00517	0.00518
			AEst	0.89800	0.90904	0.90917	0.90904	0.90890	0.90904	0.90894
30	18	4	RMSE	0.02797	0.00560	0.00562	0.00560	0.00559	0.00560	0.00560
			MRAB	0.02266	0.00498	0.00500	0.00498	0.00495	0.00498	0.00496
			AEst	0.89444	0.90902	0.90916	0.90902	0.90889	0.90902	0.90892
30	23	2	RMSE	0.03194	0.00581	0.00582	0.00581	0.00581	0.00581	0.00581
			MRAB	0.02711	0.00517	0.00518	0.00517	0.00517	0.00517	0.00517
			AEst	0.89002	0.90828	0.90842	0.90828	0.90814	0.90828	0.90818
30	23	3	RMSE	0.03466	0.00470	0.00470	0.00470	0.00471	0.00470	0.00471
			MRAB	0.02854	0.00420	0.00420	0.00420	0.00419	0.00420	0.00419
			AEst	0.89919	0.90971	0.90984	0.90971	0.90958	0.90971	0.90961
30	23	4	RMSE	0.02559	0.00486	0.00490	0.00486	0.00483	0.00486	0.00484
			MRAB	0.02279	0.00434	0.00439	0.00434	0.00430	0.00434	0.00431
			AEst	0.89243	0.90931	0.90942	0.90931	0.90920	0.90931	0.90923
60	35	2	RMSE	0.02772	0.00616	0.00618	0.00616	0.00615	0.00616	0.00615
			MRAB	0.02372	0.00564	0.00566	0.00564	0.00563	0.00564	0.00563
			AEst	0.89726	0.90978	0.90988	0.90978	0.90968	0.90978	0.90971
60	35	3	RMSE	0.02084	0.00583	0.00586	0.00583	0.00581	0.00583	0.00582
			MRAB	0.01809	0.00518	0.00522	0.00518	0.00515	0.00518	0.00516
			AEst	0.89959	0.90825	0.90834	0.90825	0.90815	0.90825	0.90817
60	35	4	RMSE	0.02075	0.00508	0.00508	0.00508	0.00508	0.00508	0.00508
			MRAB	0.01797	0.00446	0.00447	0.00446	0.00446	0.00446	0.00446
			AEst	0.89705	0.90880	0.90891	0.90880	0.90870	0.90880	0.90873
60	45	2	RMSE	0.02126	0.00534	0.00534	0.00534	0.00534	0.00534	0.00534
			MRAB	0.01839	0.00483	0.00485	0.00483	0.00482	0.00483	0.00482
			AEst	0.89702	0.90905	0.90915	0.90905	0.90895	0.90905	0.90897
60	45	3	RMSE	0.02235	0.00552	0.00553	0.00552	0.00551	0.00552	0.00551
			MRAB	0.01904	0.00491	0.00493	0.00491	0.00489	0.00491	0.00490
			AEst	0.90024	0.91002	0.91012	0.91002	0.90992	0.91002	0.90995
60	45	4	RMSE	0.02255	0.00572	0.00574	0.00572	0.00569	0.00572	0.00570
			MRAB	0.01905	0.00545	0.00548	0.00545	0.00542	0.00545	0.00543
			AEst	0.89978	0.91025	0.91034	0.91025	0.91016	0.91025	0.91018
90	50	2	RMSE	0.02032	0.00618	0.00621	0.00618	0.00616	0.00618	0.00617
			MRAB	0.01712	0.00585	0.00587	0.00585	0.00583	0.00585	0.00584
			AEst	0.89897	0.90857	0.90865	0.90857	0.90849	0.90857	0.90851
90	50	3	RMSE	0.02046	0.00611	0.00611	0.00611	0.00611	0.00611	0.00611
			MRAB	0.01749	0.00550	0.00552	0.00550	0.00549	0.00550	0.00549
			AEst	0.89973	0.90777	0.90785	0.90777	0.90769	0.90777	0.90771
90	50	4	RMSE	0.01888	0.00564	0.00563	0.00564	0.00565	0.00564	0.00565
			MRAB	0.01661	0.00503	0.00502	0.00503	0.00503	0.00503	0.00503
			AEst	0.89814	0.90810	0.90819	0.90810	0.90801	0.90810	0.90804
90	65	2	RMSE	0.02038	0.00520	0.00519	0.00520	0.00521	0.00520	0.00521
			MRAB	0.01775	0.00472	0.00472	0.00472	0.00473	0.00472	0.00473
			AEst	0.90045	0.90983	0.90991	0.90983	0.90975	0.90983	0.90977
90	65	3	RMSE	0.02020	0.00554	0.00556	0.00554	0.00552	0.00554	0.00553
			MRAB	0.01664	0.00508	0.00510	0.00508	0.00506	0.00508	0.00507
			AEst	0.89877	0.90673	0.90681	0.90673	0.90665	0.90673	0.90667
90	65	4	RMSE	0.01929	0.00520	0.00517	0.00520	0.00522	0.00520	0.00522
			MRAB	0.01698	0.00443	0.00441	0.00443	0.00445	0.00443	0.00444

Table 5. Results of the point estimate for $h(t = 0.15)$ under H-T-II CS.

						LINEXLF			GELF	
n	r	τ		MLE	SELF	$c = -3$	$c = 0.0001$	$c = 3$	$q = -1$	$q = 1$
			AEst	0.69914	0.62106	0.62906	0.62106	0.61334	0.62106	0.61268
30	18	2	RMSE	0.24250	0.04412	0.04395	0.04412	0.04567	0.04412	0.04638
			MRAB	0.29607	0.05598	0.05514	0.05598	0.05878	0.05598	0.05974
			AEst	0.70733	0.62609	0.63362	0.62609	0.61881	0.62609	0.61825
30	18	3	RMSE	0.20344	0.04356	0.04419	0.04356	0.04421	0.04356	0.04482
			MRAB	0.25676	0.05486	0.05614	0.05486	0.05494	0.05486	0.05568
			AEst	0.69555	0.62232	0.62942	0.62232	0.61542	0.62232	0.61485
30	18	4	RMSE	0.19732	0.04176	0.04164	0.04176	0.04304	0.04176	0.04365
			MRAB	0.22536	0.05355	0.05216	0.05355	0.05575	0.05355	0.05656
			AEst	0.71071	0.62270	0.63004	0.62269	0.61557	0.62270	0.61501
30	23	2	RMSE	0.21279	0.04370	0.04405	0.04370	0.04457	0.04370	0.04519
			MRAB	0.25799	0.05595	0.05609	0.05595	0.05737	0.05595	0.05819
			AEst	0.74320	0.62819	0.63561	0.62819	0.62099	0.62819	0.62045
30	23	3	RMSE	0.23214	0.03512	0.03613	0.03512	0.03566	0.03512	0.03615
			MRAB	0.27213	0.04519	0.04554	0.04519	0.04652	0.04519	0.04719
			AEst	0.68389	0.61728	0.62425	0.61728	0.61052	0.61728	0.60990
30	23	4	RMSE	0.17383	0.03665	0.03529	0.03665	0.03915	0.03665	0.03976
			MRAB	0.22060	0.04723	0.04462	0.04723	0.05130	0.04723	0.05218
			AEst	0.71671	0.62033	0.62644	0.62033	0.61439	0.62033	0.61389
60	35	2	RMSE	0.17629	0.04569	0.04526	0.04569	0.04688	0.04569	0.04743
			MRAB	0.21396	0.06014	0.05937	0.06014	0.06151	0.06014	0.06222
			AEst	0.69511	0.61570	0.62109	0.61570	0.61044	0.61570	0.60996
60	35	3	RMSE	0.13820	0.04389	0.04277	0.04389	0.04559	0.04389	0.04612
			MRAB	0.17331	0.05664	0.05407	0.05664	0.05995	0.05664	0.06069
			AEst	0.68545	0.62611	0.63130	0.62611	0.62104	0.62611	0.62067
60	35	4	RMSE	0.14228	0.03795	0.03807	0.03795	0.03852	0.03795	0.03890
			MRAB	0.17686	0.04833	0.04780	0.04833	0.04980	0.04833	0.05034
			AEst	0.69484	0.62286	0.62839	0.62286	0.61748	0.62286	0.61707
60	45	2	RMSE	0.13659	0.04052	0.04057	0.04052	0.04122	0.04052	0.04165
			MRAB	0.17083	0.05320	0.05217	0.05320	0.05529	0.05320	0.05593
			AEst	0.69836	0.62082	0.62621	0.62082	0.61557	0.62082	0.61514
60	45	3	RMSE	0.14946	0.04176	0.04139	0.04176	0.04280	0.04176	0.04325
			MRAB	0.18218	0.05384	0.05245	0.05384	0.05582	0.05384	0.05642
			AEst	0.67669	0.61357	0.61884	0.61357	0.60844	0.61357	0.60797
60	45	4	RMSE	0.15401	0.04357	0.04235	0.04357	0.04534	0.04357	0.04584
			MRAB	0.18595	0.05993	0.05763	0.05993	0.06265	0.05993	0.06336
			AEst	0.67294	0.61251	0.61734	0.61251	0.60779	0.61251	0.60734
90	50	2	RMSE	0.13124	0.04627	0.04497	0.04627	0.04798	0.04627	0.04847
			MRAB	0.16104	0.06278	0.06133	0.06278	0.06439	0.06278	0.06501
			AEst	0.68502	0.62323	0.62756	0.62323	0.61899	0.62323	0.61867
90	50	3	RMSE	0.13695	0.04564	0.04553	0.04564	0.04615	0.04564	0.04652
			MRAB	0.16671	0.05996	0.05883	0.05996	0.06133	0.05996	0.06186
			AEst	0.68450	0.62802	0.63222	0.62802	0.62391	0.62802	0.62363
90	50	4	RMSE	0.12926	0.04167	0.04195	0.04167	0.04182	0.04167	0.04213
			MRAB	0.16237	0.05317	0.05369	0.05317	0.05314	0.05317	0.05352
			AEst	0.68883	0.62715	0.63176	0.62715	0.62264	0.62715	0.62233
90	65	2	RMSE	0.13298	0.03931	0.03973	0.03931	0.03944	0.03931	0.03975
			MRAB	0.16579	0.05145	0.05189	0.05145	0.05176	0.05145	0.05219
			AEst	0.67625	0.61370	0.61796	0.61370	0.60954	0.61370	0.60916
90	65	3	RMSE	0.13521	0.04260	0.04146	0.04260	0.04409	0.04260	0.04449
			MRAB	0.16088	0.05614	0.05459	0.05614	0.05810	0.05614	0.05864
			AEst	0.69193	0.63567	0.63993	0.63567	0.63150	0.63567	0.63128
90	65	4	RMSE	0.13348	0.03753	0.03864	0.03753	0.03690	0.03753	0.03714
			MRAB	0.16732	0.04610	0.04716	0.04610	0.04564	0.04610	0.04595

Table 6. Results of the interval estimates for α, β, λ, $S(t = 0.15)$, and $h(t = 0.15)$ under H-T-II CS.

				α		β		λ		$S(t)$		$h(t)$	
n	r	τ		MLE	Bayesian	MLE	Bayesian	MLE	Bayesian	MLE	Bayesian	MLE	Bayesian
30	18	2	AL	1.3300	0.2871	3.0676	0.1449	1.5373	0.0215	0.1519	0.0388	0.9747	0.2832
			CP	0.953	0.988	0.963	0.971	0.950	0.971	0.947	0.976	0.956	0.982
30	18	3	AL	1.1463	0.2789	1.9466	0.1393	0.7008	0.0211	0.1372	0.0377	0.9166	0.2747
			CP	0.957	0.989	0.966	0.972	0.952	0.975	0.950	0.991	0.959	0.983
30	18	4	AL	0.9994	0.2726	1.3005	0.1310	0.3484	0.0202	0.1233	0.0367	0.8440	0.2674
			CP	0.963	0.999	0.967	0.997	0.968	0.986	0.966	0.995	0.963	0.994
30	23	2	AL	1.1007	0.2787	1.8176	0.1349	0.7171	0.0206	0.1349	0.0376	0.9168	0.2740
			CP	0.948	0.975	0.933	0.974	0.946	0.977	0.969	0.985	0.966	0.982
30	23	3	AL	1.1222	0.2753	1.7065	0.1360	0.5733	0.0205	0.1316	0.0371	0.8858	0.2704
			CP	0.949	0.981	0.940	0.989	0.963	0.981	0.972	0.997	0.975	0.993
30	23	4	AL	0.9773	0.2692	1.2196	0.1304	0.3282	0.0200	0.1210	0.0363	0.8289	0.2637
			CP	0.957	0.992	0.956	0.996	0.971	0.982	0.974	0.997	0.976	0.994
60	35	2	AL	0.9682	0.2523	2.2812	0.1390	1.1396	0.0216	0.1107	0.0340	0.7070	0.2478
			CP	0.921	0.984	0.924	0.974	0.933	0.983	0.925	0.979	0.938	0.982
60	35	3	AL	0.7947	0.2386	1.3006	0.1292	0.4444	0.0211	0.0960	0.0322	0.6406	0.2332
			CP	0.955	0.989	0.925	0.977	0.934	0.985	0.936	0.982	0.959	0.988
60	35	4	AL	0.6968	0.2353	0.8779	0.1232	0.2288	0.0198	0.0865	0.0315	0.5916	0.2287
			CP	0.958	0.999	0.945	0.992	0.963	0.994	0.943	0.994	0.961	0.999
60	45	2	AL	0.8006	0.2414	1.3874	0.1301	0.5402	0.0208	0.0960	0.0324	0.6382	0.2355
			CP	0.949	0.975	0.932	0.973	0.932	0.976	0.934	0.989	0.935	0.972
60	45	3	AL	0.7691	0.2390	1.1767	0.1274	0.3844	0.0206	0.0935	0.0321	0.6291	0.2331
			CP	0.952	0.986	0.952	0.977	0.941	0.995	0.950	0.991	0.938	0.986
60	45	4	AL	0.7350	0.2367	1.0802	0.1258	0.3434	0.0204	0.0900	0.0318	0.6064	0.2303
			CP	0.958	0.987	0.958	0.987	0.950	0.997	0.966	0.995	0.961	0.989
90	50	2	AL	0.7724	0.2260	1.8607	0.1333	0.9357	0.0218	0.0889	0.0305	0.5612	0.2211
			CP	0.952	0.973	0.956	0.981	0.943	0.974	0.954	0.982	0.941	0.978
90	50	3	AL	0.6481	0.2155	1.0718	0.1267	0.3680	0.0213	0.0784	0.0289	0.5216	0.2090
			CP	0.956	0.981	0.958	0.982	0.950	0.977	0.961	0.983	0.959	0.981
90	50	4	AL	0.5647	0.2145	0.6974	0.1193	0.1785	0.0200	0.0703	0.0286	0.4810	0.2069
			CP	0.970	0.998	0.963	0.992	0.952	0.983	0.970	0.988	0.963	0.989
90	65	2	AL	0.6908	0.2212	1.3333	0.1291	0.5598	0.0213	0.0820	0.0297	0.5370	0.2152
			CP	0.945	0.974	0.943	0.972	0.940	0.988	0.944	0.977	0.945	0.985
90	65	3	AL	0.6277	0.2153	0.9790	0.1243	0.3192	0.0212	0.0764	0.0288	0.5112	0.2076
			CP	0.946	0.974	0.950	0.979	0.942	0.989	0.959	0.995	0.946	0.993
90	65	4	AL	0.5702	0.2144	0.7121	0.1200	0.1835	0.0199	0.0708	0.0287	0.4850	0.2071
			CP	0.967	0.985	0.958	0.986	0.945	0.991	0.970	0.999	0.948	0.997

Table 7. COVID-19 mortality rates in the United Kingdom.

0.0587	0.0863	0.1165	0.1247	0.1277	0.1303	0.1652	0.2079	0.2395	0.2751	0.2845
0.2992	0.3188	0.3317	0.3446	0.3553	0.3622	0.3926	0.3926	0.4110	0.4633	0.4690
0.4954	0.5139	0.5696	0.5837	0.6197	0.6365	0.7096	0.7193	0.7444	0.8590	1.0438
1.0602	1.1305	1.1468	1.1533	1.2260	1.2707	1.3423	1.4149	1.5709	1.6017	1.6083
1.6324	1.6998	1.8164	1.8392	1.8721	1.9844	2.1360	2.3987	2.4153	2.5225	2.7087
2.7946	3.3609	3.3715	3.7840	3.9042	4.1969	4.3451	4.4627	4.6477	5.3664	5.4500
5.7522	6.4241	7.0657	7.4456	8.2307	9.6315	10.1870	11.1429	11.2019	11.4584	

Table 8. COVID-19 mortality rates in Albania.

0.785	1.376	1.560	1.825	1.969	1.984	2.083	2.976	3.214	3.268	3.646
3.723	3.846	3.846	3.922	4.348	4.571	4.730	4.762	4.762	5.446	5.607
5.622	6.726	6.842	7.692	7.772	8.025	8.638	8.696	8.936	9.416	10.407
10.714	11.188	11.538	11.719	11.804	12.268	12.527	12.644	12.967	13.018	13.110
13.690	13.807	13.903	13.984	14.211	14.912	14.925	15.224	15.484	15.929	15.971
16.190	16.197	16.409	16.86	17.296	17.486	17.536	17.607	17.788	17.913	18.269
18.312	18.561	18.725	19.149	19.557	19.568	19.647	19.926	19.939	19.940	20.034
20.124	20.574	21.127	21.481	21.898	21.951	21.953	21.959	22.118	22.543	23.214
24.059	24.211	24.299	24.947	25.554	26.411	26.667	26.683	26.904	27.915	30.667
30.672	33.708	34.356	35.149	49.718						

Half-Logistic Distribution (PHLD) proposed by Krishnarani [32], and the Generalized Rayleigh distribution (GRD) introduced by Raqab and Madi [42]. The PDFs of these competing distributions are presented below.

1. LLD(α,β) : $f(y;\alpha,\beta) = \alpha\beta^{-\alpha}y^{\alpha-1}\left(1+\left(\frac{y}{\beta}\right)^{\alpha}\right)^{-2}, \alpha,\beta>0.$
2. IELD(α,β,λ) : $f(y;\alpha,\beta,\lambda) = \frac{\alpha\beta\lambda}{y^2}(1+\frac{\beta}{y})^{-\alpha-1}\left(1-(1+\frac{\beta}{y})^{-\alpha}\right)^{\lambda-1}, \alpha,\beta,\lambda>0.$
3. WGD(α,β,λ) : $f(y;\alpha,\beta,\lambda) = \frac{\beta\lambda}{\alpha}y^{\lambda-1}\left(\frac{y^{\lambda}}{\alpha}+1\right)^{-(\beta+1)}, \alpha,\beta,\lambda>0.$
4. LOD(α,β) : $f(y;\alpha,\beta) = \alpha\beta(1+\beta y)^{-(\alpha+1)}, \alpha,\beta>0.$
5. APIWD(α,β,λ) : $f(y;\alpha,\beta,\lambda) = \frac{\beta\lambda\log(\alpha)}{\alpha-1}y^{-(\beta+1)}e^{-\lambda y^{-\beta}}\alpha^{e^{-\lambda y^{-\beta}}}, \alpha,\beta,\lambda>0.$
6. WD(α,β) : $f(y;\alpha,\beta) = \frac{\beta}{\alpha}\left(\frac{y}{\alpha}\right)^{(\beta-1)}e^{-\left(\frac{y}{\alpha}\right)^{\beta}}, \alpha,\beta>0.$
7. LHRD(α,β) : $f(y;\alpha,\beta) = (\alpha+\beta y)e^{-\left(\alpha y+\frac{\beta}{2}y^2\right)}, \alpha,\beta>0.$
8. PHLD(α,β) : $f(y;\alpha,\beta) = 2\alpha\beta y^{\beta-1}e^{\alpha y^{\beta}}\left(1+e^{\alpha y^{\beta}}\right)^{-2}, \alpha,\beta>0.$
9. GRD(α,β) : $f(y;\alpha,\beta) = \frac{2\alpha^{\beta+1}}{\Gamma(\beta+1)}e^{\alpha\left(-y^2\right)}y^{2\beta+1}, \alpha>0,\beta>-1.$

The findings of the goodness-of-fit tests and model comparisons are presented in Tables 9 and 10. These findings indicate that the CDF of the QHRD fits the dataset effectively, as it has the highest P-value, that surpasses 0.05. This suggests that the QHRD outperforms the alternatives evaluated. Significant values are highlighted in **bold** for emphasis. As a result, we accept the null hypothesis that the theoretical and sample distributions are identical. Also, a visual comparison was conducted between the empirical CDF and the fitted CDFs for the QHRD and competing distributions across both datasets to determine the QHRD fit more accurately. Additionally, a histogram with the fitted PDFs was generated for these distributions. Furthermore, P-P plots and Q-Q plots were also generated to further assess the QHRD fit, as illustrated in Figure 3. Both the visual analysis and goodness-of-fit tests consistently demonstrate that the QHRD provides a superior fit to both datasets compared to the competing models.

In this study, observing all events over a prolonged period is impractical. To overcome this limitation, we apply H-T-II CS, as outlined in subsection 1.1, by focusing our analysis on data available up to max $(y_{r:n}, \tau)$. Specifically, we consider the H-T-II CS as $(n, r, \tau) = (76, 40, 1.82)$ for COVID-19 mortality rates in the United Kingdom at $t = 0.15$ and $(104, 45, 14)$ for those in Albania at $t = 2$. Therefore, the corresponding censored data values for both datasets are presented in Tables 11 and 12. The point and interval estimates obtained through the classical method (ML) for both datasets are presented in Tables 13, 14, and 15 along

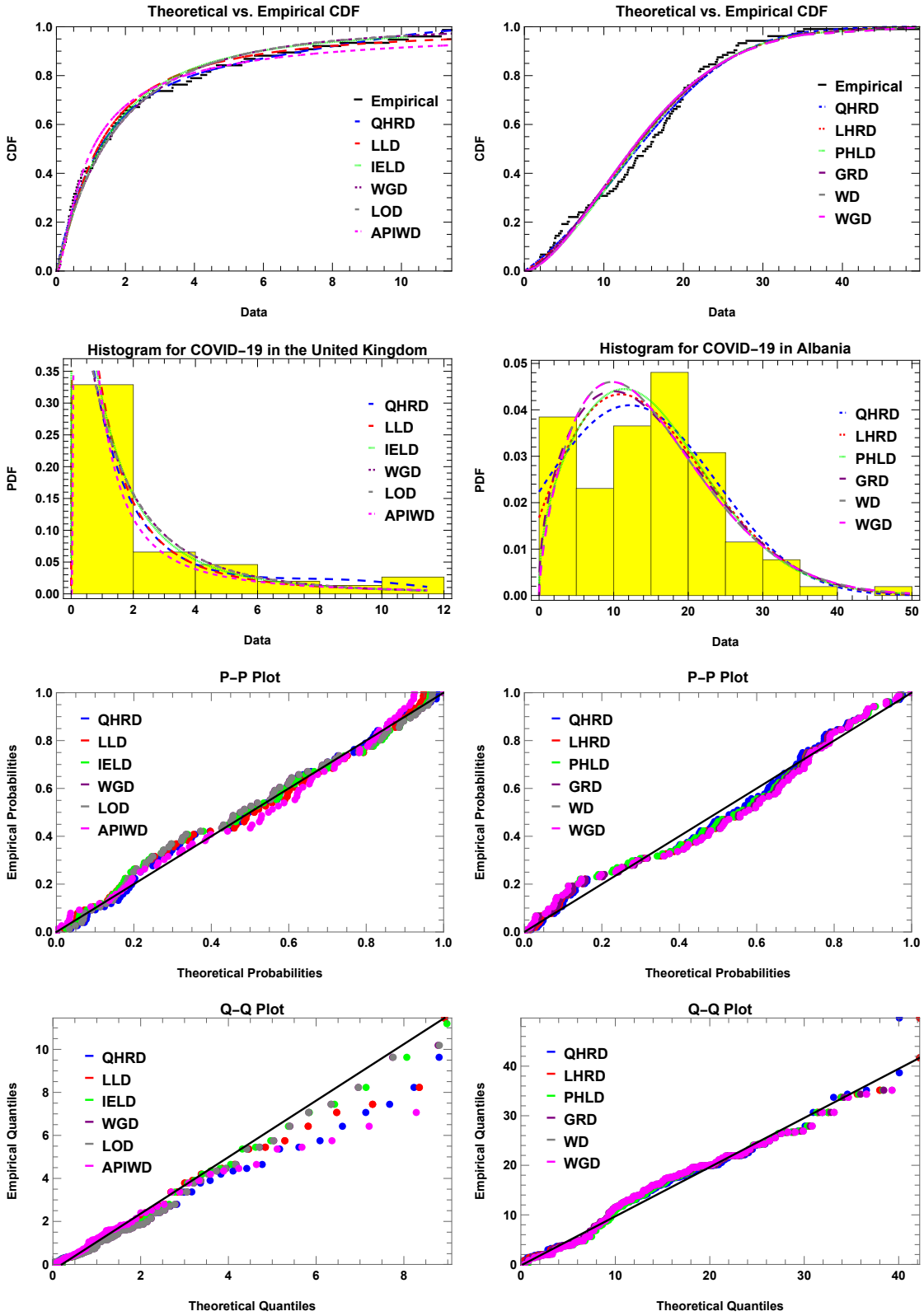

Figure 3. Empirical and Fitted CDFs **(top row)**, Histogram with Fitted PDFs **(upper-middle row)**, P-P plots **(lower-middle row)**, and Q-Q plots **(bottom row)** for COVID-19 mortality rates in the United Kingdom **(left)** and Albania **(right)**.

Table 9. Goodness-of-fit results of the QHRD and others for COVID-19 mortality rates in the United Kingdom.

	MLE(St.Er)										
Model	$\hat{\alpha}$	$\hat{\beta}$	$\hat{\lambda}$	-2ℓ	AIC	CAIC	BIC	HQIC	W^*	A^*	K-S (P-value)
QHRD	**0.6546(0.1008)**	**−0.1641(0.0506)**	**0.0149(0.0055)**	**276.119**	**282.119**	**282.452**	**289.111**	**284.913**	**0.0324**	**0.3000**	**0.0494(0.9880)**
LLD	1.2895(0.1208)	1.1851(0.1867)	⋯	284.472	288.472	288.637	293.134	290.335	0.0663	0.4739	0.0618(0.9164)
IELD	1.1773(0.4435)	2.5390(3.6994)	2.1625(1.5248)	282.654	288.654	288.987	295.646	291.448	0.0714	0.4957	0.0708(0.8152)
WGD	5.5627(8.9264)	3.2359(4.5434)	0.9912(0.2167)	282.861	288.861	289.194	295.853	291.655	0.0701	0.5087	0.0733(0.7815)
LOD	3.0767(1.7027)	0.1902(0.1364)	⋯	282.862	286.862	287.027	291.524	288.725	0.0703	0.5078	0.0733(0.7813)
APIWD	17.527(27.329)	0.9450(0.0822)	0.2617(0.1249)	286.04	292.04	292.374	299.033	294.835	0.0830	0.6285	0.0796(0.6906)
WD	0.8466(0.0743)	2.2200(0.3185)	⋯	283.504	287.504	287.668	292.165	289.367	0.1009	0.6969	0.0806(0.6771)

Table 10. Goodness-of-fit results of the QHRD and others for COVID-19 mortality rates in Albania.

	MLE(St.Er)										
Model	$\hat{\alpha}$	$\hat{\beta}$	$\hat{\lambda}$	-2ℓ	AIC	CAIC	BIC	HQIC	W^*	A^*	K-S (P-value)
QHRD	**0.0223(0.0112)**	**0.0030(0.0027)**	**0.0001(0.0001)**	**737.546**	**743.546**	**743.786**	**751.479**	**746.760**	**0.1023**	**0.6264**	**0.0592(0.83732)**
LHRD	0.0168(0.0077)	0.0048(0.0009)	⋯	738.119	742.119	742.238	747.408	744.262	0.1568	0.8685	0.0750(0.5764)
PHLD	0.0233(0.0089)	1.4611(0.1211)	⋯	737.098	741.098	741.217	746.387	743.241	0.1573	0.9691	0.0788(0.5126)
GRD	0.0024(0.0004)	−0.2640(0.0874)	⋯	737.897	741.897	742.016	747.186	744.039	0.1929	1.0377	0.0823(0.4574)
WD	1.6722(0.1325)	16.857(1.0365)	⋯	739.583	743.583	743.701	748.871	745.725	0.2282	1.3082	0.0877(0.3783)
WGD	$1 \times 10^6(3 \times 10^7)$	10031(266530)	1.6723(0.1325)	739.584	745.584	745.824	753.517	748.798	0.2282	1.3084	0.0877(0.3782)

with their standard error (St.Er) and 95% ACI bounds (L and U) and ALs. Also, we generated 48, 000 MCMC iterations and burned the first 8, 000. Bayesian estimates (BEs), including their standard error (St.Er) and 95% BCI bounds (L and U) and ALs, are also reported in these tables. These findings indicate that BEs obtained via MCMC are more precise than the corresponding MLEs, as evidenced by their narrower credible intervals compared to the asymptotic intervals of MLEs, further underscoring the accuracy of the Bayesian approach.

Table 11. Observed data from H-T-II on COVID-19 mortality rates in the United Kingdom.

0.0587	0.0863	0.1165	0.1247	0.1277	0.1303	0.1652	0.2079	0.2395	0.2751	0.2845
0.2992	0.3188	0.3317	0.3446	0.3553	0.3622	0.3926	0.3926	0.4110	0.4633	0.4690
0.4954	0.5139	0.5696	0.5837	0.6197	0.6365	0.7096	0.7193	0.7444	0.8590	1.0438
1.0602	1.1305	1.1468	1.1533	1.2260	1.2707	1.3423	1.4149	1.5709	1.6017	1.6083
1.6324	1.6998	1.8164								

Table 12. Observed data from H-T-II on COVID-19 mortality rates in Albania.

0.785	1.376	1.560	1.825	1.969	1.984	2.083	2.976	3.214	3.268	3.646
3.723	3.846	3.846	3.922	4.348	4.571	4.730	4.762	4.762	5.446	5.607
5.622	6.726	6.842	7.692	7.772	8.025	8.638	8.696	8.936	9.416	10.407
10.714	11.188	11.538	11.719	11.804	12.268	12.527	12.644	12.967	13.018	13.110
13.690	13.807	13.903	13.984							

According to the Bayesian results from COVID-19 mortality rates in the United Kingdom, $S(t = 0.15) =$

Table 13. Point estimates for α, β, λ, $S(t)$, and $h(t)$ from COVID-19 mortality rates in the United Kingdom.

			LINEXLF(St.Er)			GELF(St.Er)	
Par.	MLE(St.Er)	SELF(St.Er)	$c = -3$	$c = 0.0001$	$c = 3$	$q = -1$	$q = 1$
α	0.7094(0.2449)	0.6480(0.0606)	0.6536(0.0609)	0.6480(0.0606)	0.6426(0.0608)	0.6480(0.0606)	0.6424(0.0609)
β	−0.3565(0.6647)	−0.1905(0.0354)	−0.1886(0.0354)	−0.1905(0.0354)	−0.1924(0.0354)	−0.1905(0.0354)	−0.1832(0.0361)
λ	0.1292(0.3554)	0.0202(0.0054)	0.0202(0.0054)	0.0202(0.0054)	0.0201(0.0054)	0.0202(0.0054)	0.0187(0.0056)
$S(0.15)$	0.9025(0.2449)	0.9093(0.0082)	0.9094(0.0082)	0.9093(0.0082)	0.9092(0.0082)	0.9093(0.0082)	0.9093(0.0082)
$h(0.15)$	0.6589(0.6647)	0.6199(0.0595)	0.6253(0.0597)	0.6199(0.0595)	0.6147(0.0597)	0.6199(0.0595)	0.6142(0.0597)

Table 14. Point estimates for α, β, λ, $S(t)$, and $h(t)$ from COVID-19 mortality rates in Albania.

			LINEXLF(St.Er)			GELF(St.Er)	
Par.	MLE(St.Er)	SELF(St.Er)	$c = -3$	$c = 0.0001$	$c = 3$	$q = -1$	$q = 1$
α	0.0284(0.0187)	0.0499(0.0069)	0.0500(0.0069)	0.0499(0.0069)	0.0499(0.0069)	0.0499(0.0069)	0.0490(0.0070)
β	0.0015(0.0067)	−0.0036(0.0013)	−0.0036(0.0013)	−0.0036(0.0013)	−0.0036(0.0013)	−0.0036(0.0013)	−0.0029(0.0014)
λ	0.0001(0.0005)	0.0001(0.0001)	0.0001(0.0001)	0.0001(0.0001)	0.0001(0.0001)	0.0001(0.0001)	0.0001(0.0001)
$S(2)$	0.9417(0.0187)	0.9113(0.0113)	0.9115(0.0113)	0.9113(0.0113)	0.9111(0.0113)	0.9113(0.0113)	0.9111(0.0113)
$h(2)$	0.0318(0.0067)	0.0432(0.0058)	0.0433(0.0058)	0.0432(0.0058)	0.0432(0.0058)	0.0432(0.0058)	0.0425(0.0057)

Table 15. Interval estimates for α, β, λ, $S(t)$, and $h(t)$ from COVID-19 mortality rates in the United Kingdom and Albania.

	United Kingdom						Albania					
	MLE			Bayesian			MLE			Bayesian		
Par.	L	U	AL	L	U	AL	L	U	AL	L	U	AL
α	0.2294	1.1894	0.9600	0.5315	0.7696	0.2381	−0.0083	0.0651	0.0733	0.0368	0.0637	0.0269
β	−1.6592	0.9462	2.6054	−0.2600	−0.1217	0.1384	−0.0116	0.0147	0.0263	−0.0059	−0.0010	0.0049
λ	−0.5673	0.8257	1.3930	0.0096	0.0305	0.0209	−0.0008	0.0010	0.0018	0.0000	0.0002	0.0002
$S(t)$	0.8485	0.9566	0.1081	0.8924	0.9244	0.0321	0.8926	0.9908	0.0982	0.8895	0.9336	0.0441
$h(t)$	0.3309	0.9869	0.6560	0.5093	0.7423	0.2331	0.0138	0.0497	0.0359	0.0325	0.0545	0.0221

0.90 and $h(t = 0.15) = 0.62$, implying that out of 100 patients diagnosed or hospitalized with COVID-19, approximately 90 are expected to survive beyond $t = 0.15$ time units. Among all patients who reach $t = 0.15$ time units, their chance of deterioration or death stands at 62% per unit time. The patient shows good chances of survival, although healthcare providers must remain watchful due to their ongoing moderate risk of death or health decline. Similarly, according to the Bayesian results from COVID-19 mortality rates in Albania, $S(t = 2) = 0.91$ and $h(t = 2) = 0.04$, implying that out of 100 patients diagnosed or hospitalized with COVID-19, approximately 91 are expected to survive beyond $t = 2$ time units. At $t = 2$ time units, for those who have already survived up to this time point, the instantaneous risk of deterioration or mortality is 4% per unit time. This indicates that while the patient has a high probability of having survived to this point and a relatively low risk, patients are likely to remain stable, although not entirely free from risk, and it underscores the importance of ongoing clinical observation and intervention, especially for high-risk individuals.

For improving the accuracy and reliability of parameter estimates for both datasets, we construct profile log-likelihood curves and their first partial derivatives based on Equations (2.2)–(2.5). We also generate contour plots of the log-likelihood function for the MLEs. Figures 4 and 5 display the profile log-likelihood curves with their first partial derivatives, while Figures 6 and 7 show the corresponding contour plots. These results confirm the existence and uniqueness of the MLEs, as the respective functions reach their maximum at these estimates. To assess the convergence of the MCMC samplers under H-T-II CS for the datasets, we present the trace plots, their convergence, and Gaussian kernel density estimates in Figures 8 and 9. These figures also include histogram plots of α, β, and λ, as well as $S(t)$ and $h(t)$. The sample mean is indicated by a dashed blue line, while the 95% confidence interval bounds are marked by connected blue lines in each plot. The results shown in Figures 8 and 9 demonstrate that the MCMC samplers have converged appropriately and that the posterior estimates are nearly symmetric. Overall, the point and interval estimates in Tables 13, 14, and 15 indicate that BEs consistently exhibit superior performance, as they have the lowest St.Er and AL.

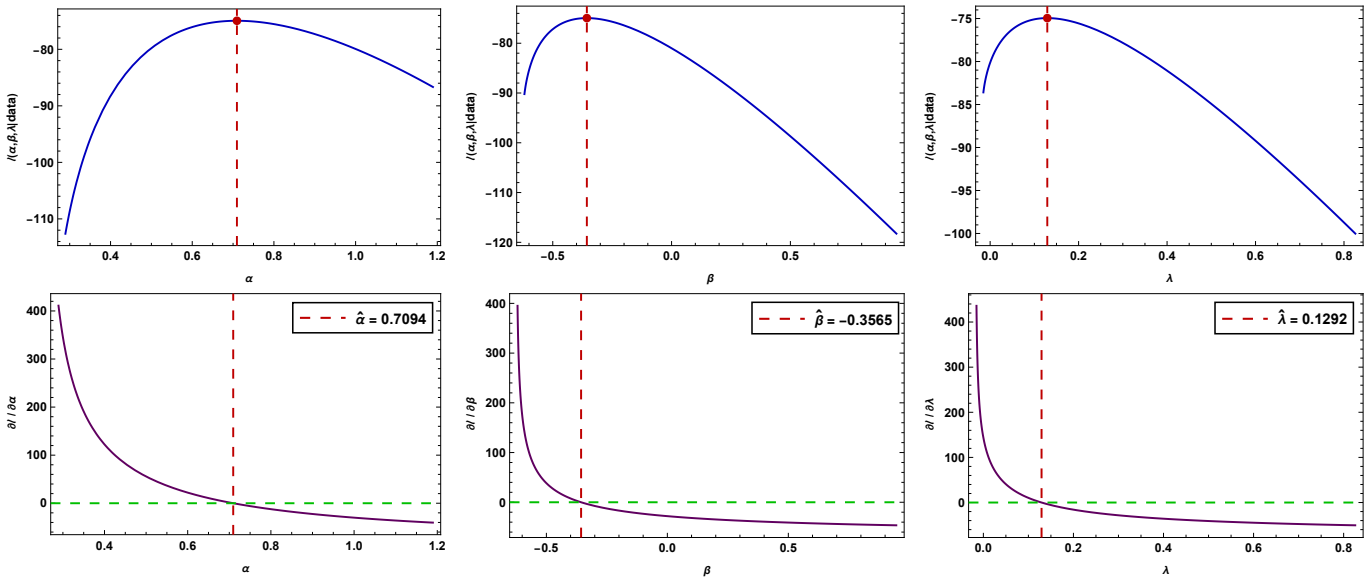

Figure 4. Profile log-likelihood functions **(blue curves, top)** and their first partial derivatives **(purple curves, bottom)** for the parameters α, β, and λ, including the MLEs (**big red point**) for COVID-19 mortality rates in the United Kingdom.

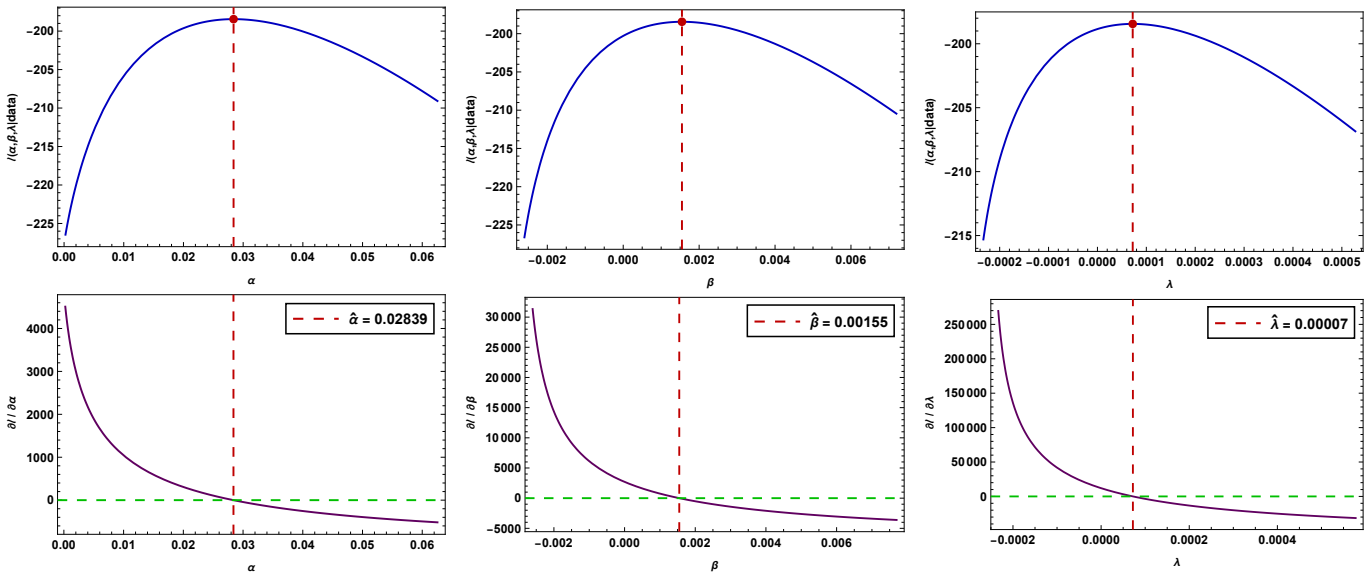

Figure 5. Profile log-likelihood functions **(blue curves, top)** and their first partial derivatives **(purple curves, bottom)** for the parameters α, β, and λ, including the MLEs (**big red point**) for COVID-19 mortality rates in Albania.

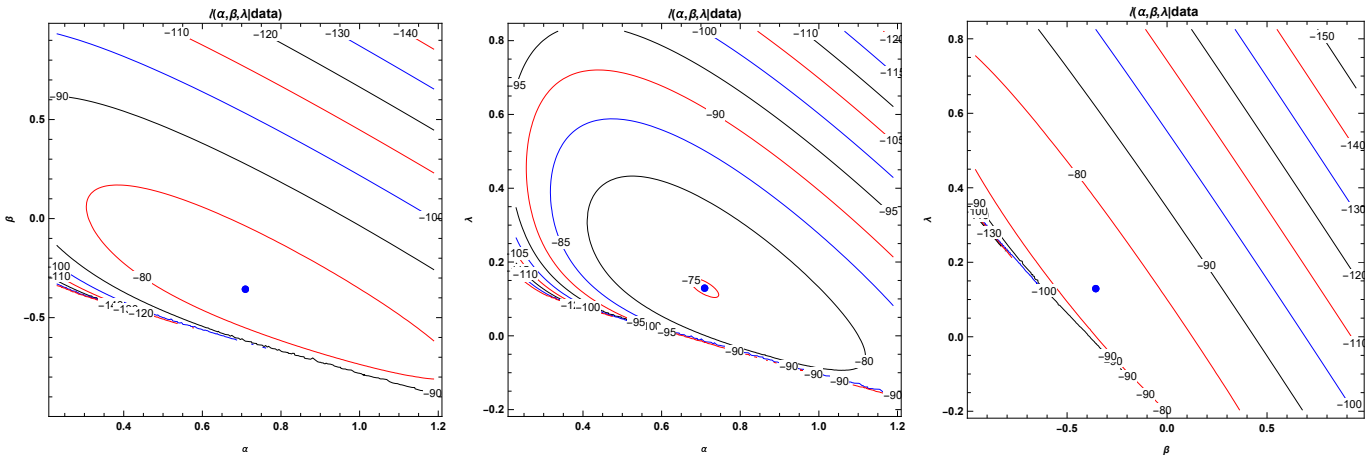

Figure 6. Contour plots of the log-likelihood function for the parameters α, β, and λ, along with the global maximum for COVID-19 mortality rates in the United Kingdom.

6. Conclusion

This study demonstrated the effectiveness of the hybrid Type-II censoring scheme (H-T-II CS) in estimating the unknown parameters, survival, and hazard rate functions of the quadratic hazard rate distribution (QHRD), addressing gaps in some lifetime data, and providing cost-effective testing alternatives. Both non-Bayesian and Bayesian estimation approaches were explored. In the non-Bayesian context, the maximum likelihood estimation (MLE) method was used to derive point estimates and asymptotic confidence intervals, utilizing the observed Fisher information matrix for parameters and the delta method for survival and hazard rate functions. The Bayesian framework provided point estimates and highest posterior density

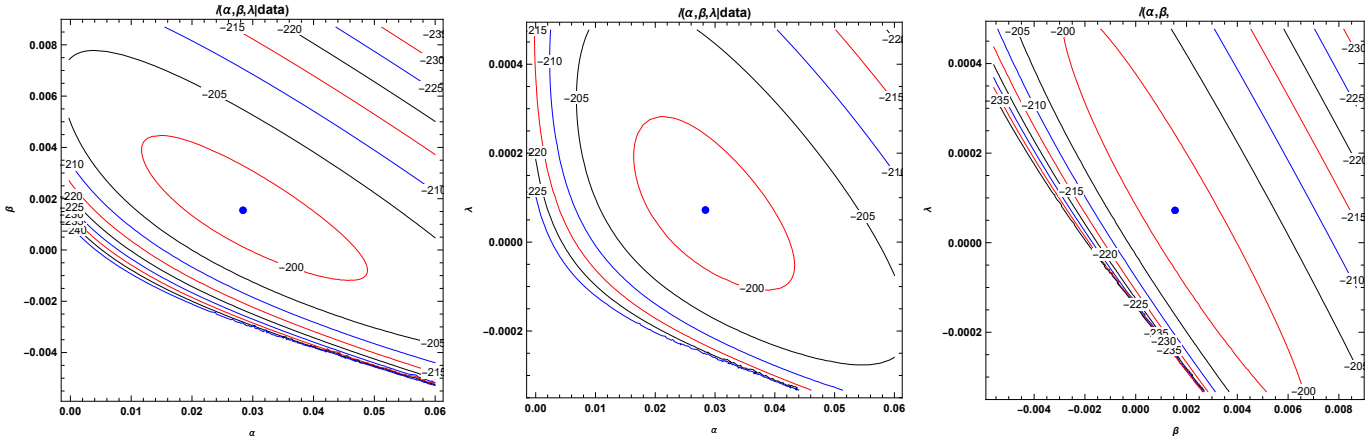

Figure 7. Contour plots of the log-likelihood function for the parameters α, β, and λ, along with the global maximum for COVID-19 mortality rates in Albania.

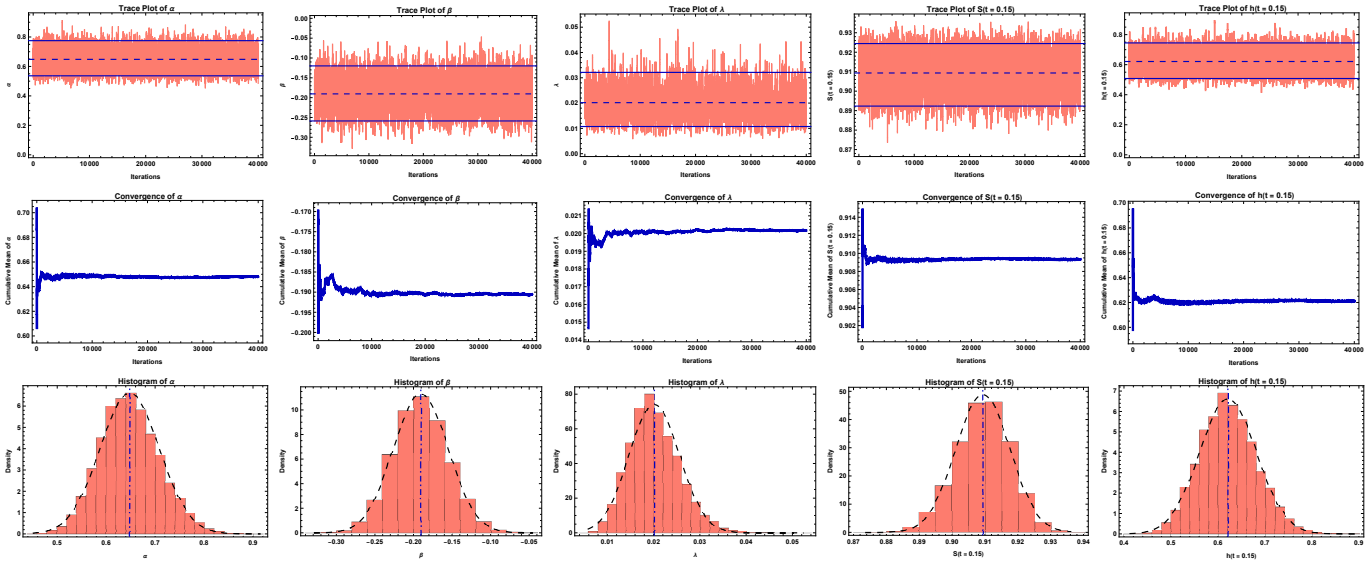

Figure 8. MCMC trace plots **(top)** and its convergence **(center)** along with histogram and proposal distribution (normal) plots **(bottom)** for the MLEs of α, β, λ, $S(t)$, and $(h(t)$ for COVID-19 mortality rates in the United Kingdom.

(HPD) credible intervals under the MLE method, using independent informative priors: gamma priors for parameters α and λ and a normal prior for β. These estimates were obtained using symmetric (squared error) and asymmetric (linear exponential and general entropy) loss functions via MCMC simulation due to the lack of explicit analytical solutions. A simulation study was conducted across varying sample sizes (n), the predetermined number of failures (r), and the predetermined time (τ) to assess the accuracy, robustness, and applicability of the distribution in modeling lifetime data. The practical utility of the methods was further validated with two real-life medical datasets on COVID-19 mortality rates from different regions after fitting it to the QHRD and comparing its performance with some competing models. The results indicated that the QHRD outperforms its alternatives, making it the most suitable replacement. Furthermore, we investigated both the uniqueness and existence of the estimates before verifying their status through graphical methods to confirm they represent the unique and global maximum. Additionally, we confirmed

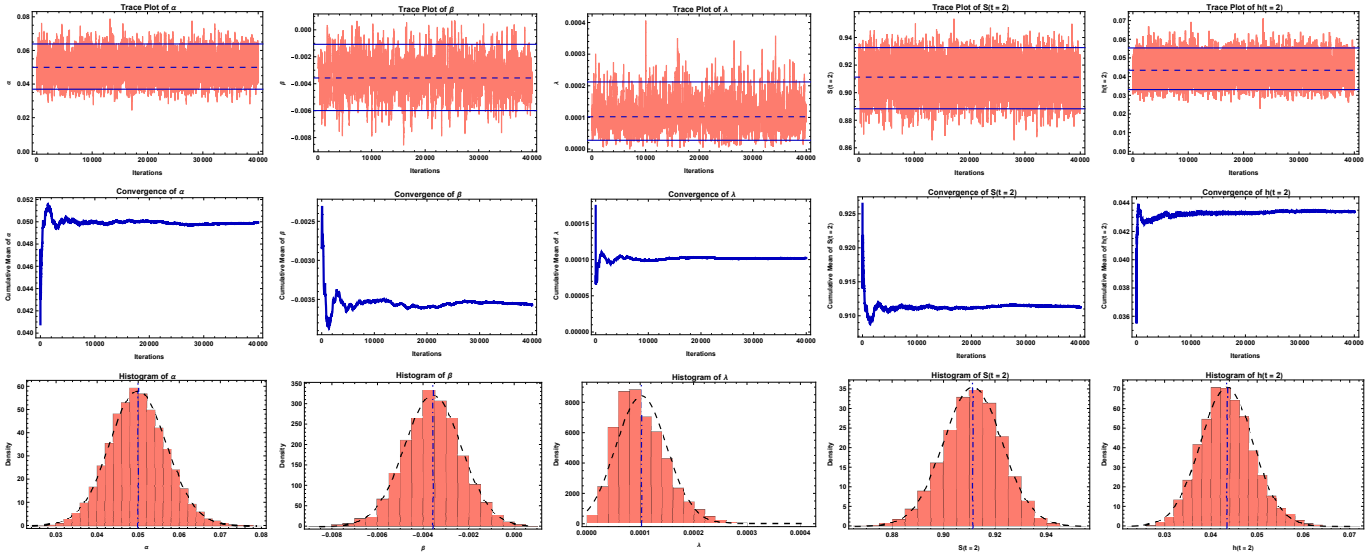

Figure 9. MCMC trace plots **(top)** and its convergence **(center)** along with histogram and proposal distribution (normal) plots **(bottom)** for the MLEs of α, β, λ, $S(t)$, and $(h(t)$ for COVID-19 mortality rates in Albania.

the convergence, accuracy, and reliability of the estimates by making some graphical plots. Based on the results, particularly the RMSE, MRAB, AL, and CP metrics, we recommend the Bayesian method as a robust approach for estimating unknown parameters and the survival and hazard rate functions of the QHRD using H-T-II CS. Overall, this study improves accuracy levels combined with efficiency in estimating parameters when dealing with H-T-II CS, thus providing clinicians and researchers a reliable tool for risk assessment, patient monitoring, and informed decision-making in critical care settings.

7. Future Work

This study establishes a comprehensive foundation for the implementation of the H-T-II CS within both Bayesian and non-Bayesian estimation frameworks. Nevertheless, several directions remain open for further investigation to extend and strengthen the current findings. Future research may focus on the following areas:

1. **Broader applicability:** Expanding the use of the proposed methods through real-world applications in engineering, electronics, and healthcare reliability studies, supported by the development of specialized computational tools.
2. **Comparative analyses:** Conducting systematic comparisons between Bayesian, frequentist, and alternative Bayesian estimation approaches—such as the Tierney–Kadane and E-Bayesian estimators—along with a thorough assessment of prior distribution selection and its influence on estimation accuracy.
3. **Methodological extensions:** Extending the current framework to accommodate more advanced censoring structures, including adaptive and generalized hybrid schemes, as well as accelerated and partially accelerated life testing (ALT and PALT) under varying stress levels.
4. **Model robustness:** Enhancing model performance under sparse or incomplete data conditions by

integrating informative priors and employing posterior predictive validation techniques.

5. **Model generalization:** Investigating multivariate and mixture formulations to better capture systems characterized by multiple failure modes or heterogeneous populations.

These prospective directions are expected to enrich both the theoretical development and practical applicability of Bayesian inference under complex censoring environments, leading to more accurate, flexible, and generalizable reliability modeling frameworks.

Authors' Contributions

All authors have worked equally to write and review the manuscript.

Data Availability Statement

The data that supports the findings of this study are available within the article.

Conflicts of Interest

The authors declare no conflict of interest.

References

1.Al-Hossain, A. and Dar, J. (2016). Some results on moment of order statistics for the quadratic hazard rate distribution. *J. Stat. Appl. Probab.*, 5:371–376.

2.Alghamdi, A. S. and Abd El-Raouf, M. M. (2023). Exploring the dynamics of covid-19 with a novel family of models. *Mathematics*, 11:1641.

3.Almongy, H., Almetwally, E., Aljohani, H., Alghamdi, A., and Hossam, E. (2021). A new extended rayleigh distribution with applications of covid-19 data. *Results in Physics*, 23:104012.

4.Almuqrin, M., Gemeay, A., Abd El-Raouf, M., Kilai, M., Aldallal, R., and Hossam, E. (2022). A flexible extension of reduced kies distribution: Properties, inference, and applications in biology. *Complexity*, 2022:1–19.

5.Althubyani, F., Abd El-Bar, A. M. T., Fawzy, M. A., and Gemeay, A. (2022). A new 3-parameter bounded beta distribution: Properties, estimation, and applications. *Axioms*, 11:504.

6.Atchadé, M. N., N'bouké, M., Djibril, A., Shahzadi, S., Hossam, E., Aldallal, R., Alshanbari, H. M., Gemeay, A., and El-Bagoury, A. A. (2023). A new power topp–leone distribution with applications to engineering and industry data. *PLOS ONE*, 18:e0278225.

7.Ateya, S. (2015). Estimation under inverse weibull distribution based on balakrishnan's unified hybrid censored scheme. *Communications in Statistics - Simulation and Computation*.

8.Azzalini, A. (1996). *Statistical Inference Based on the Likelihood*. Chapman & Hall, London.

9.Bain, L. J. (2017). *Statistical Analysis of Reliability and Life-Testing Models: Theory and Methods*. CRC Press, Boca Raton.

10.Banerjee, A. and Kundu, D. (2008). Inference based on type-ii hybrid censored data from a weibull distribution. *IEEE Transactions on Reliability*, 57(2):369–378.

11.Basheer, A. M. (2019). Alpha power inverse weibull distribution with reliability application. *J. Taibah Univ. Sci.*, 13(1):423–432.

12.Bhatti, F. A., Hamedani, G. G., Sheng, W., and Ahmad, M. (2018). On extended quadratic hazard rate distribution: Development, properties, characterizations, and applications. *Stochastics and Quality Control*, 33(1):45–60.

13.Calabria, R. and Pulcini, G. (1994). An engineering approach to bayes estimation for the weibull distribution. *Microelectronics Reliability*, 34(5):789–802.

14.Childs, A., Chandrasekar, B., Balakrishnan, N., and Kundu, D. (2003). Exact likelihood inference based on type-i and type-ii hybrid censored samples from the exponential distribution. *Annals of the Institute of Statistical Mathematics*, 55:319–330.

15.Dey, S., Dey, T., and Luckett, D. (2015). Statistical inference for the generalized inverted exponential distribution based on upper record values. *Math. Comput. Simul.*, 120.

16.Du, K., Wang, M., Lu, T., and Sun, X. (2021). Estimation based on hybrid censored data from the power lindley distribution. *Communications in Statistics - Simulation and Computation*.

17.Dube, S., Pradhan, B., and Kundu, D. (2011). Parameter estimation of the hybrid censored log-normal distribution. *Journal of Statistical Computation and Simulation*, pages 275–287.

18.Eissa, F. Y. and Sonar, C. D. (2024). Extended odd weibull–lindley distribution. *AIP Adv.*, 14:035317.

19.El-Sagheer, R. (2018). Estimation of parameters of weibull–gamma distribution based on progressively censored data. *Stat. Papers*, 59.

20.EL-Sagheer, R. M., Eliwa, M. S., Alqahtani, K. M., and EL-Morshedy, M. (2022). Asymmetric randomly censored mortality distribution: Bayesian framework and parametric bootstrap with application to covid-19 data. *Journal of Mathematics*, 2022:8300753.

21.Elbatal, I. and Butt, N. S. (2014). A new generalization of quadratic hazard rate distribution. *Pak. J. Stat. Oper. Res.*, 9(4):343–361.

22.Eliason, S. R. (1993). *Maximum Likelihood Estimation: Logic and Practice*, volume 96. SAGE Publications, Newbury Park, CA.

23.Elmorsy, R. and Hassan, A. (2019). Parameter estimation for inverted exponentiated lomax distribution with right censored data. *Gazi Univ. J. Sci.*, 2019(32):1370–1386.

24.Ganguly, A., Mitra, S., Samanta, D., and Kundu, D. (2012). Exact inference for the two-parameter exponential distribution under type-ii hybrid censoring. *Journal of Statistical Planning and Inference*, pages 613–625.

25.Gilks, W. R., Richardson, S., and Spiegelhalter, D. (1995). *Markov Chain Monte Carlo in Practice*. Chapman & Hall/CRC, New York.

26.Greene, W. H. (2002). *Econometric Analysis*. Prentice Hall, Upper Saddle River, 5th edition.

27.Gupta, R. and Kundu, D. (1998). Hybrid censoring schemes with exponential failure distribution. *Communications in Statistics-Theory and Methods*, 27:3065–3083.

28.Held, L. and Sabanés Bové, D. (2014). *Applied Statistical Inference: Likelihood and Bayes*. Springer, Berlin, Heidelberg.

29.Hossam, E., Abdulrahman, A., Gemeay, A., Alshammari, N., and Alshawarbeh, E. (2022). A novel extension of gumbel distribution: Statistical inference with covid-19 application. *Alexandria Engineering Journal*, 61.

30.Jaheen, Z. (2004). Empirical bayes inference for generalized exponential distribution based on records. *Commun. Stat. - Theory Methods*, 33:1851–1861.

31.Kohansal, A. and Rezakhah, S. (2012). Parameter estimation of type-ii hybrid censored weighted exponential distribution. *Communications in Statistics - Simulation and Computation*.

32.Krishnarani, S. D. (2016). On a power transformation of half-logistic distribution. *J. Prob. Stat.*, 2016:1–10.

33.Kundu, D. (2007). On hybrid censored weibull distribution. *Journal of Statistical Planning and Inference*, 137:2127–2142.

34.Liang, T. and Yang, M. C. (2011). Optimal bayesian sampling plans for exponential distributions based on hybrid censored samples. *Journal of Statistical Computation and Simulation*.

35.Lin, C. T., Huang, Y. L., and Balakrishnan, N. (2008). Exact bayesian variable sampling plans for the exponential distribution based on type-i and type-ii hybrid censored samples. *Communications in Statistics-Simulation and Computation*, 37:1101–1116.

36.Lynch, S. M. (2007). *Introduction to Applied Bayesian Statistics and Estimation for Social Scientists*. Springer Science & Business Media, Berlin.

37.Mansour, M. M. M. and Aboshady, M. S. (2022). Assessing the performance of insulating fluids via point of statistical inference view. *TWMS Journal of Applied and Engineering Mathematics*, 2022:469–480.

38.Merovci, F. and Elbatal, I. (2015). The beta quadratic hazard rate distribution. *Pak. J. Stat.*, 31:427–446.

39.Mustafa, A. (2016). A new bivariate distribution with generalized quadratic hazard rate marginals. *J. Math. Stat.*, 12(4):255–270.

40.Nadarajah, S. and Kotz, S. (2007). A class of generalized models for shadowed fading channels. *Wireless Pers. Commun.*, 43:1113–1120.

41.Okasha, H., Kayid, M., Abouammoh, A., and Elbatal, I. (2016). A new family of quadratic hazard rate-geometric distributions with reliability applications. *J. Testing Eval.*, 44:20150116.

42.Raqab, M. Z. and Madi, M. T. (2011). Inference for the generalized rayleigh distribution based on progressively censored data. *J. Stat. Plan. Inference*, 141(10):3313–3322.

43.Rasekhi, M., Saber, M. M., Hamedani, G. G., Abd El-Raouf, M. M., Aldallal, R., and Gemeay, A. M. (2022). Approximate maximum likelihood estimations for the parameters of the generalized gudermannian distribution and its characterizations. *J. Math.*, 2022:4092576.

44.Singh, S. and Tripathi, Y. (2018). Estimating the parameters of an inverse weibull distribution under progressive type-i interval censoring. *Stat. Papers*, 59:21–56.

45.Singh, V. P. (1998). *Two-Parameter Log-Logistic Distribution*. Springer Netherlands, Dordrecht.

46.Slater, J. J., Bansal, A., Campbell, H., Rosenthal, J. S., Gustafson, P., and Brown, P. E. (2023). A bayesian approach to estimating covid-19 incidence and infection fatality rates. *Biostatistics*, 25:354–384.

47.Tierney, L. (1994). Markov chains for exploring posterior distributions. *Ann. Stat.*, 22:1701–1728.

48.Weibull, W. (2021). A statistical distribution function of wide applicability. *J. Appl. Mech.*, 18(3):293–297.

49.Yadav, A. S., Singh, S. K., and Singh, U. (2016). Bayes estimator of the parameter and reliability function of marshall-olkin extended exponential distribution using hybrid type-ii censored data. *Journal of Statistics and Management Systems*, pages 325–344.

50.Zellner, A. (1986). Bayesian estimation and prediction using asymmetric loss functions. *J. Am. Stat. Assoc.*, 81:446–451.